UNIVERSIDADE DE SÃO PAULO
ESCOLA DE ENGENHARIA DE SÃO CARLOS

Jorge Romero Rodríguez

Analysis of the Effects of Boundary Layer Ingestion on Fan Performance Using CFD

São Carlos

2025

Jorge Romero Rodríguez

Analysis of the Effects of Boundary Layer Ingestion on Fan Performance Using CFD

Monografia apresentada ao Curso de Engenharia Aeronáutica, da Escola de Engenharia de São Carlos da Universidade de São Paulo, como parte dos requisitos para obtenção do título de Engenheiro Aeronáutico.

Advisor: Paulo Celso Greco Jr.

São Carlos

2025

Cataloging-in-publication data prepared by the Prof. Sérgio Rodrigues Fontes Library and the Communication and Marketing Office at EESC-USP, with information provided by the author.

R532a

Romero Rodríguez, Jorge

Analysis of the Effects of Boundary Layer Ingestion on Fan Performance Using CFD / Jorge Romero Rodríguez ; advisor Paulo Celso Greco Jr.. -- São Carlos, 2025.

75 p.

Undergraduate Thesis in Aeronautical Engineering -- São Carlos School of Engineering of University of São Paulo, 2025.

1. CFD. 2. Boundary Layer Ingestion. 3. Wind tunnel Tests. 4. Aerodynamic Fan. 5. Turbulence. I. Paulo Celso, Greco Jr., advisor. II. Título.

Responsible for the cataloging structure of the publication according to AACR2: EESC Librarians

FOLHA DE APROVAÇÃO
Approval sheet

Candidato / *Student*: Jorge Romero Rodríguez
Título do TCC / *Title* : Analysis of the Effects of Boundary Layer Ingestion on Fan Performance Using CFD
Data de defesa / *Date*: 26/09/2025

Comissão Julgadora / *Examining committee*	**Resultado** / *result*
Professor Associado Paulo Celso Greco Junior	APROVADO
Instituição / Affiliation: EESC - SAA	
Professor Associado Hernan Dario Cerón Muñoz	APROVADO
Instituição / Affiliation: EESC - SAA	
Professor Doutor Alvaro Martins Abdalla	APROVADO
Instituição / Affiliation: EESC - SAA	

Presidente da Banca / Chair of the Examining Committee:

Professor Associado Paulo Celso Greco Junior
(assinatura / *signature*)

Dedicated to my family and friends,
whose support has been essential to all my accomplishments.

ACKNOWLEDGEMENTS

I would like to take this opportunity to thank everyone who, in one way or another, have made this work possible and have supported me on this journey.

First and foremost, to my advisor, Paulo Greco, for his guidance, patience, and for everything he has taught me throughout this entire process. His advice has been key to the succesful completion of this work.

My gratitude also goes to my home university in Spain, the University Carlos III Madrid, for training me as an aerospace engineer and giving me the opportunity to spend this unforgettable year in the Universidade de São Paulo, where I also learned so much from its professors.

To my family, my parents María Rodríguez Ordoñez and Jorge Romero Santaescolástica, and especially to my grandmother Isabel Santaescolástica. Thank you for your unconditional support, for teaching the most important things in life, and for always being my pillar. This accomplishment is as much yours as it is mine.

And, of course, to my Brazilian home, República Berlim. Thank you for taking me in and integrating me as one of your own from the very first day I arrived in São Carlos. The moments we have shared, the support, and the friendship you have given me have made this year an experience I will never forget.

To all of you, thank you very much.

"Sometimes, flying feels too divine for human accomplishment. Sometimes, the world seen from above seems too beautiful, too wonderful, too distant for human eyes to see."

Charles A. Lindbergh

ABSTRACT

Romero Rodríguez, J. **Analysis of the Effects of Boundary Layer Ingestion on Fan Performance Using CFD**. 2025. 75 p. Monograph (Conclusion Course Paper) - Escola de Engenharia de São Carlos, Universidade de São Paulo, São Carlos, 2025.

In this study, the impact of boundary layer ingestion (BLI) on the performance of an aircraft fan has been analyzed using CFD simulations. The research was divided in two phases. First, a set of wind tunnel configurations were evaluated to determine the most effective geometry for generating a consistent turbulent boundary layer. The second part consisted on using the most suitable configuration to evaluate the effects of this phenomenon on key fan parameters. The results for thrust, torque, fan efficiency, static and total pressure variation and the pressure distribution on the rotor blade were then compared to those of a conventional clean configuration. This analysis provides valuable insights into the benefits and challenges of BLI, which could guide towards potential improvements for its future physical implementation.

Keywords: CFD. Boundary Layer Ingestion. Wind tunnel Tests. Aerodynamic Fan. Turbulence. Propulsive Efficiency. Pressure Distribution.

RESUMO

Romero Rodríguez, J. **Analysis of the Effects of Boundary Layer Ingestion on Fan Performance Using CFD**. 2025. 75 p. Monografia (Trabalho de Conclusão de Curso) - Escola de Engenharia de São Carlos, Universidade de São Paulo, São Carlos, 2025.

Neste estudo, o impacto da ingestão da camada limite (BLI) no desempenho de um fan de aeronave foi analisado usando simulações CFD. A pesquisa foi dividida em duas fases. Primeiro, um conjunto de configurações de túnel de vento foi avaliado para determinar a geometria mais eficaz para gerar uma camada limite turbulenta consistente. A segunda parte consistiu em utilizar a configuração mais adequada para avaliar os efeitos desse fenômeno nos principais parâmetros do fan. Os resultados de empuxo, torque, eficiência do fan, variação de pressão estática e total e distribuição de pressão na pá do rotor foram então comparados aos de uma configuração limpa convencional. Esta análise fornece informações valiosas sobre os benefícios e desafios do BLI, que podem orientar para potenciais melhorias em sua futura implementação física.

Palavras-chave: CFD. Ingestão da Camada Limite. Testes em Túnel de Vento. Fan Aerodinâmico. Turbulência. Eficiência Propulsiva. Distribuição de Pressão.

LIST OF FIGURES

LIST OF TABLES

LIST OF ABBREVIATIONS AND ACRONYMS

BL	Boundary Layer
BLI	Boundary Layer Ingestion
WI	Wake Ingestion
CFD	Computational Fluid Dynamics
PSC	Power Saving Coefficient
AFC	Active Flow Control
BWB	Blended Winged-Body
PBM	Power Balance Method
BPR	By-Pass Ratio
SFC	Specific Fuel Consumption
AIP	Aerodynamic Interface Plane
VTP	Vertical Tail Plane
PFC	Propulsive Fuselage Concept
ANCF	Active Noise Control Fan
ICD	Inlet Control Device
RANS	Reynolds-Averaged Navier-Stokes
DNS	Direct Numerical Simulation
TKE	Turbulence Kinetic Energy

LIST OF SYMBOLS

P_p	Propulsive Power $[W]$
P'_p	Propulsive Power without WI $[W]$
η_p	Propulsive Efficiency
$\dot{m}$	Mass Flow Rate $[kg/s]$
ρ	Density $[Kg/m^3]$
$\bar{\rho}$	Averaged Density $[Kg/m^3]$
ρ'	Fluctuating Density $[Kg/m^3]$
T	Temperature $[K]$
μ	Dynamic viscosity $[kg/ms]$
P_s	Static Pressure $[Pa]$
P_t	Total Pressure $[Pa]$
η_{fan}	Fan Efficiency
F	Thrust $[N]$
ω	Angular Velocity $[rad/s]$
τ	Torque $[N \cdot m]$

CONTENTS

1 INTRODUCTION

Throughout the modern era, aviation has stood as one of the main drivers of technological advancement, fostering a global air connectivity network that enables the rapid movement of people and goods across the world. Continuous innovations in aerodynamics, materials and propulsion systems have helped to develop the marvel of modern aviation, jet engines. These engines have transformed air travel, replacing piston engines and allowing aircraft to reach higher speeds, altitudes and ranges.

Back in the 1930s, Frank Whittle in the United Kingdom and Hans von Ohain in Germany independently initiated the development of turbojet engines. While Whittle is credited with the first patent, von Ohain successfully developed and tested the first functional turbojet, paving the way for turbine-powered flight. Despite revolutionizing high-speed flight, these early engines still exhibited drawbacks such as elevated specific fuel consumption and limited propulsive efficiency during subsonic operation. Although they continue to serve as the workhorse of modern-day commercial aviation, these limitations motivated the development of turbofan architectures. Turbofans are characterized by a ducted fan stage which enables them to provide a greater thrust and a higher propulsor efficiency throughout all phases of flight, while also reducing acoustic emissions. At present, turbofan engines persist as the dominant powerplant technology for the majority of civil aviation aircraft.

Despite their high efficiency, in practical applications, the aerodynamic environment surrounding the aircraft often influences the airflow entering the engine, causing it to operate under non-ideal conditions. One of the most significant phenomena occurs when the airflow passes along the fuselage surface and forms a boundary layer of slower, turbulent air which is later ingested by the engine. This boundary layer ingestion (BLI) causes alterations in the velocity profile and has a significant impact in the engine performance.

1.1 Introduction to turbofans

Turbofans are a type of jet engine that consist of a large fan at the front part which receives the incoming airflow and splits it into two streams. One stream is directed into the core, where it is compressed, mixed with the fuel, and combusted, while the other goes around the core through a bypass duct generating a significant share of the total thrust. These engines are one of the most popular propulsion systems in modern commercial aviation since they combine the high-speed capabilities of turbojets with improved efficiency and reduced noise (Sarkar, 2006).

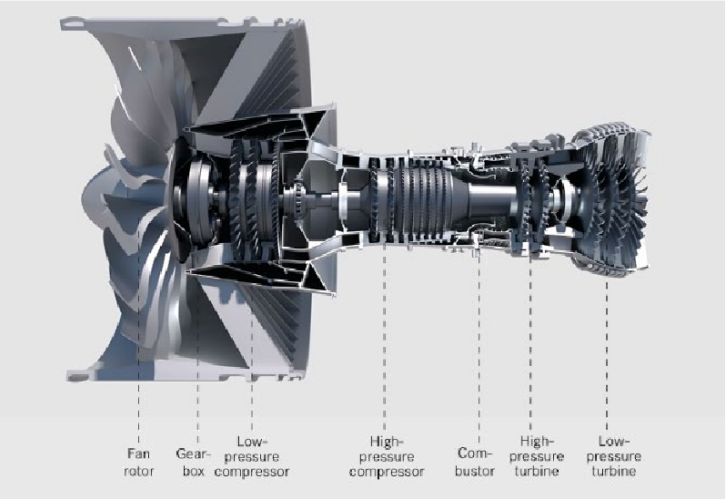

Figure 1 – Turbofan architecture (Wei, 2023)

The main advantage of turbofans lies in the integration of a ducted fan stage combined with an increased bypass ratio which enhances propulsive efficiency and leads to lower fuel burn and reduced acoustic emissions. In this way, this configuration effectively overcomes the limitations of turbojets. These higher bypass ratios, however, require larger fan diameters which lead to weight problems, often addressed by the use of lightweight materials. Ongoing research is exploring effective techniques to further reduce turbofan noise and study the phenomena of boundary layer ingestion.

1.2 Introduction to BLI

Boundary layer ingestion (BLI) is a promising technology currently under investigation, expected to attain multiple design goals including improved energy efficiency and reduced noise emissions for the next generation of commercial aircraft. The concept is mainly based on embedding the engine within fuselage so that it ingests the boundary layer generated along the airframe body. While theoretical studies indicate potential performance benefits, BLI also introduces new operational and design challenges for turbofan integration.

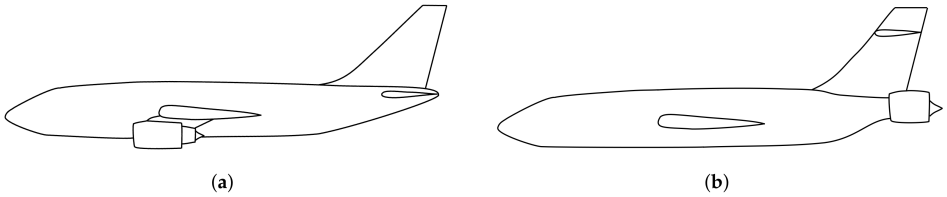

Figure 2 – (a) Aircraft with conventional propulsor; (b) Aircraft with BLI propulsor (Diamantidou D.E.; Hosain, 2022)

The boundary layer developing over the fuselage and wing areas generates a non-uniform velocity profile which exhibits a momentum and energy deficit. This low-energy

fluid, participates in engine work and contributes to a more efficient flight. Recent studies indicate that, in contrast with traditional propulsion, BLI configurations leverage this low-momentum inflow combined with its compact integration to reduce the airframe drag and fuel consumption, while enhancing overall efficiency.

In particular, low-momentum inflow helps to compensate the velocity deficit in the aircraft's wake , reducing the overall aerodynamic drag and lowering the energy losses in the exhaust wake (Lv *et al.*, 2016a). As a result, less power is needed to generate the same thrust under identical flight conditions, leading to lower fuel consumption and improved overall eficiency (Diamantidou D.E.; Hosain, 2022). Furthermore, it is worth mentioning that this lower fuel consumption enables this type of systems to offer significant reduction in pollutant emissions (Pardo; Hall, 2021a).

Although BLI offers some interesting performance benefits, it also presents several challenges that must be addressed for practical implementation. When investigating BLI propulsors, it was observed that the aerodynamics of the aircraft's fuselage is closely coupled with the system's performance. The reduced momentum flux of the ingested flow combined with the altered surface forces brings about the need for an updated force accounting method to properly determine the additional power needed by the propulsor to mantain a given thrust requirement.

Another aspect to account for are the non-uniform and unsteady inflow conditions that may lead radial and circumferential distortions at the fan degrading engine performance (Diamantidou D.E.; Hosain, 2022).

In this context, it is of interest to determine the behaviour of BLI at high supersonic speeds and if it will improve or hinder perfomance and operational limits.

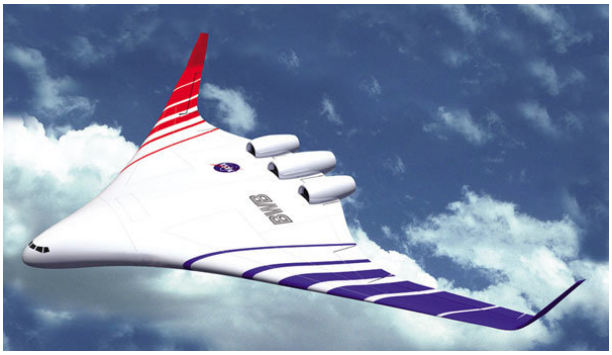

Figure 3 – BWB aircraft (Leifsson, 2006)

The Blended Wing Body (BWB) shown in the figure above, is a great example of a plane designed for BLI (Kawai; Friedman; Serrano, 2006) . Instead of having the wings separated from the fuselage, BWB consists on one big, flat body that produces lift. This highly efficient design creates a massive surface area in which embedded engines can be

easily installed. Consequently, by ingesting slow moving air, these aircrafts are expected to significantly reduce drag and make flying way more efficient.

1.3 Introduction to CFD

In order to understand how turbofan performance is compromised when ingesting boundary layer and to investigate methods for improving overall propulsion efficiency, it is essential to employ experimental tools such as wind tunnels. In this project, the aim is to develop methods to replicate in the wind tunnel a boundary layer similar to that ocurring under real flight conditions. Due to the high economic cost associated with testing various methods through multiple wind tunnel experiments, computational tools are commonly used, as in this study with Ansys ICEM CFD.

Computational Fluid Dynamics (CFD) is refered to a set of computational methods that enable to solve the coupled nonlinear equations that govern fluid motion (mass, momentum and energy) (Bhattacharyya John P. Abraham, 2022). At the beginning, CFD could only handle relatively simple problems, two-dimensional, incompressible and steady-state situations often limited to laminar flows. Over time, this tool evolved, enabling the resolution of more complex three-dimensional problems which involved turbulence, compressibility effects, and unsteady flow conditions, thus becoming an indispensable resource in modern aerodynamic analysis.

Despite this progress, no practical computational model is capable of fully resolving turbulence in real engineering applications, which makes turbulence modeling an essential aspect of CFD. For the present case, ANSYS CFD is employed, which uses a RANS-based turbulence model, which does not directly resolve all turbulent scales but models their effect on the mean flow by averaging the governing equations. Although the results inevitably depend on the accuracy of the chosen turbulence model, this greatly reduces computational costs while still providing reliable predictions for many engineering applications (Menter; Lechner; Matyushenko, 2021).

In the context of this work, CFD is applied to simulate a wind tunnel environment in which a boundary layer profile similar to that experienced in real flight conditions is generated. By using this tool before physical testing, it is possible to evaluate the analysis of turbofan under BLI scenarios reducing the number of costly and time-consuming experimental trials.

1.4 Objectives

This thesis focuses on anlyzing the effects of turbulent boundary layer ingestion on fan performance. To study the phenomenon, an scaled model of a wind tunnel was created using the software Ansys CFD, in which modifications were introduced to obtain the desired flow characteristics. This program employed advanced equations together with adequate turbulence models to accurately describe the properties and consequences of the induced boundary layer.

The analysis of the fan's performance was conducted by comparing a configuration with BLI to a standard, clean configuration. The specific objectives of this thesis were to:

- Evaluate the most effective method for inducing a realistic boundary layer.
- Analyze the variations in key performance parameters: thrust, torque and fan efficiency.
- Examine the total and static pressure gains across the BLI fan.
- Study the distribution of forces on the rotor blades.

The comparison of these results provides insights into the effects of this phenomenon and the validated the simulation methodology. Additionally, it offers ideas for future adjustments and improvements to better represent real flight conditions and enable a physical implementation of this experiment.

2 LITERATURE REVIEW

2.1 Historical Background

The integration of propulsion systems within the airframe has been a recurring topic in aircraft design since 1947. Early studies by Smith and Roberts started exploring the idea of embedding engines inside the fuselage or wings, considering the benefits of boundary layer ingestion to reduce aerodynamic drag and improve propulsive efficiency (Smith; Roberts, 1947). In this way, these works were among the first to compare conventional podded engines with airframe configurations subjected to boundary layer inflows, resulting in higher optimum cruise speeds and reduction in fuel consumption between 5 an 10%.

Subsequent studies carried out by NASA and Douglass Aircraft Company, showed the potential of BLI propulsion. In 1962, NASA investigated the characteristics of a 1/20 airship model with stern propellers reporting a higher propulsive efficiency compared to conventional podded systems. Later in 1970, Douglass looked at the more modest approach of rear-fuselage configuration and reported that BLI can reduce wake kinetic energy, improving propulsive efficiency by up to 10% .

This methodology was further expanded by Leroy Smith in 1993 (Smith, 1991), who estimated the potential performance gains of BLI concepts by employing the incompressible actuator disk theory. His analysis evaluated the benefits of wake ingestion, quantifying the effects of considering this viscous wake of a body as part of the propulsive power. To measure the resulting reduction in propulsive power, Smith introduced the Power Saving Coefficient (PSC), defined as:

$$\mathrm{PSC} = \frac{P'_p - P_p}{P'_p}, \tag{2.1}$$

Where the prime denotes the case without wake ingestion. The study's numerical analyses showed that power savings are greatest for small propulsor, when the propulsor is positioned in an undisturbed wake, and can be in the range of 20% under favourable conditions.

In 2006, Plas extended Leroy Smith's study and used the concept of power saving coefficient to analyze the performance of an aircraft with an embedded propulsion system with BLI and flow distortion. The research highlighted that the efficiency improvements were highly dependent on the degree of inflow distortion and consequently, on the associated fan and duct losses. It noted that BLI represents a high-risk design due to limited experience with flow distortion, and demonstrated that BLI can achieve a substantial reduction in fuel consumption compared to conventional engines (Plas *et al.*, 2007).

In this same year, Kawai, Friedman and Serrano evaluated the potential of integrated propulsion systems using BLI and Active Flow Control (AFC) on a Blended Wing Body aircraft (Kawai; Friedman; Serrano, 2006). The analysis showed that AFC prevents flow separation and can reduce inlet flow distortion, decreasing drag and system weight. The study concluded that combining BLI and AFC can achieve a fuel burn reduction of up to 10%.

For aicraft with highly integrated propulsion system, distinguisihing between thrust and drag becomes a challenge, making conventional calculation methods ineffective. To address this, Mark Drela introduced the Power Balance Method (PBM) in 2009. This approach shifted the focus of the analysis from a momentum-based control volume to the mechanical power and kinetic energy of the airflow, eliminating the need to separately define thrust and drag (Drela, 2009). This method was later used by Sato (Sato, 2012) in 2012 to to demonstrate that boundary layer ingestion (BLI) can achieve a fuel reduction of up to 11%.

From 2012 onwards, several key studies consolidated the understanding of BLI benefits. Hardin, showed through numerical simulations that BLI can provide 3-5% fuel burn savings for future N+2 aircrafts, which potentially higher benefits for advanced N+3 designs due to their greater BLI fractions (Hardin *et al.*, 2012). Around the same time, the PBM was applied to demonstrate that BLI reduces wake energy losses and increase effective propulsive efficiency, even though body-propulsor interactions can also raise viscous and pressure drag (Lv *et al.*, 2016b).

Between 2014 and 2018, experimental research was done at NASA Langley using the D8 "double-bubble" concept which provided the **first large-scale wind tunnel evidence of BLI benefits** and resulted in quantified power savings with potential total benefits up to 19% when accounting for optimized configurations (Uranga *et al.*, 2017)(Uranga *et al.*, 2018).

Inlet distortion and flow characteristics were further investigated by Lieu and Van Dam, confirming that non-uniform inflow present integration challenges and reinforcing the measurable efficiency gains. Additionally, other experimental efforts tested simplified body-fan configurations (free-stream, WI and BLI configurations for their shaft-power saving), finding power savings ranging from 18% to nearly 30% depending on setup and boundary layer conditions.

In 2019, Lord (Lord *et al.*, 2019) developed a thrust-based, performance accounting methodology for ducted, boundary layer-ingesting propulsion. This method directly breaks down the BLI benefit into its two main components: the reduction of exhaust jet and airframe wake dissipation.

The research clarified that there is not only a reduction in wake dissipation due

to the transfer of energy to the wake fluid and a smaller nacelle wetted area, but also, a decrease in jet dissipation as the propulsor ingests slower-moving fluid to generate the same thrust with a lower jet velocity.

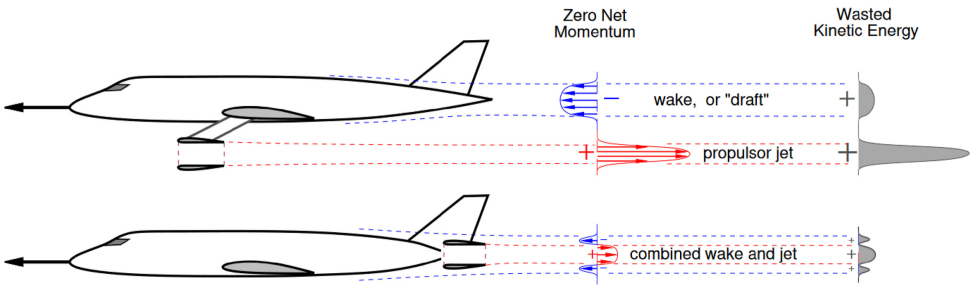

Figure 4 – Conventional vs BLI propulsor in terms of jet and wake dissipation (Ma; Lu; Li, 2025)

In recent years, research in BLI has increasingly focused on advanced computational validation, integration with new technologies such as electric propulsion, and exploration of new configurations, setting the stage for more detailed studied on performance and integration benefits.

2.2 Relevant BLI configurations with turbofans

Starting from today's highly optimized transport aircraft, the propulsion system and its synergistic integration with the airframe are expected to play a decisive role in achieving further improvements in overall efficiency. Within traditional propulsion paradigms, gains in efficiency are typically pursued by enlarging propulsor size to reduce specific thrust and thereby enhance propulsor efficiency, which introduces several integration challenges ranging from geometric constrains to structural weight penalties. Furthermore, the larger nacelles required for such propulsive devices increase wetted area, which in turn raises parasite drag and undermines vehicle efficiency. While under-wing engine installation provides structural relieve for the wing, it also has negative effects on local lift and drag characteristics. In this way, the BPR of these turbofan configurations have so far remained limited to values around 10 and 12 . Synergistic propulsion airframe integration, on the other hand, should aim to mitigate these drawbacks while fully exploiting the benefits of highly efficient power plan solucions.

Embbeded propulsion concepts also face challenges associated with inflow distortion, which variate depending on the chosen configurations and are o particular relevance in BLI. Therefore, depending on the characteristics of the non-uniform inflow and on the different aircraft configuration designs, BLI fan based propulsion systems can be further classifies into three categories shown in the figure bellow.

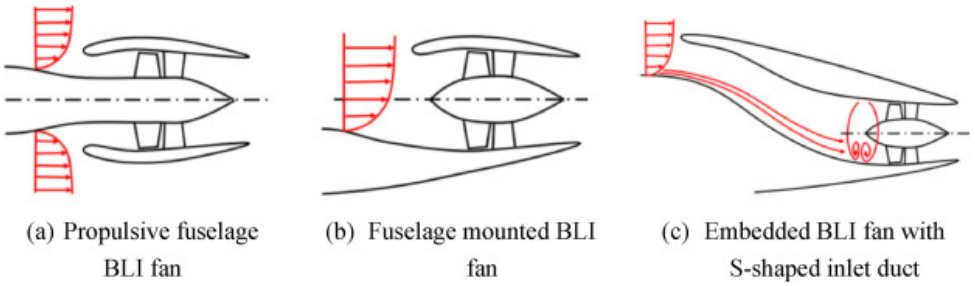

Figure 5 – Typical configurations for BLI propulsion systems (Ma; Lu; Li, 2025)

2.2.1 Propulsive Fuselage Concept (PFC)

In the first configuration, the propulsive fuselage concept (PFC), it can be observed that the fan almost uniformly ingest the boundary layer fluids of the 360º fuselage. Due to this, the circumferential non-uniformity of thje inflow can be negligible independently on the influences of the fuselage upsweep and vertical tail, making the flow to be characterized exclusively by radial distortion (Voigt; Friedrichs, 2021). This radial distortion at the Aerodynamic Interface Plane (AIP) is a consequence of a total pressure non-uniformity along the radial direction caused by the velocity deficit in the BL near the airframe surface.

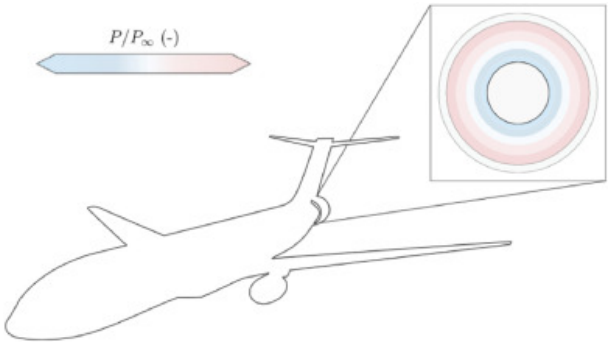

Figure 6 – Pressure distortion at AIP (Ma; Lu; Li, 2025)

However, this axisymmetric flow is only a theoretical scenario. In reality, different aircraft elements, such as the wing and vertical tail plane (VTP), introduce distortions at the fan inlet due to circulation and viscous dissipation which affect its performance. According to numerical studies (Deng *et al.*, 2023), this inflow distortion is mainly dominated by the fuselage upsweep, leading to a dependence of the total pressure coefficient on the upsweep magnitude. As the upsweep size increases, a stronger swirl is induced, which not only raises the overall drag, but also increases the fan shaft power for the fuselage-mounted configuration. Besides this contribution, inflow distortion at the fan inlet is further influenced by the fuselage boundary layer and the fuselage-tail junction. While the boundary layer around the fuselage remains circumferentially axisymmetric, the VTP introduces additional effects on the total pressure contour, arising from both the VTP viscous wake and the junction flow, which generates a low total pressure region at the core

of the horse-shoe vortex.

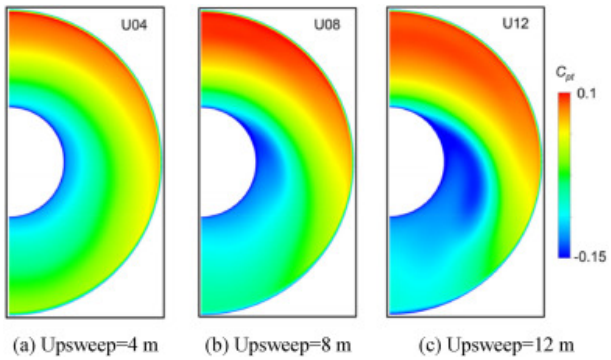

Figure 7 – VTP influence on total pressure countours (Deng *et al.*, 2023)

This configuration corresponds to conceptual aircrafts such as the STARC-ABL by NASA which uses a large electric fan embedded in the aft-part of the fuselage to ingest the boundary layer. This turbo-electric aircraft showed a 15% improvement in fuel consumption as well as significant aerodynamic and propulsive benefits (Diamantidou D.E.; Hosain, 2022).

2.2.2 Fuselage-Mounted Fans

Another relevant BLI configuration is the fuselage mounted fan configuration in which the intake recieves the airflows from the boundary layer on the aircraft surface. These type of fans have both radially and circumferentially non-uniform inlet mass flow distribution. Experimental testing and numerical simulations, have shown that the distorted inflow presents a continuous radial variation and gradient covering the entire blade height of the rotor. Additionally, low-energy fluids induced by the wall secondary flows were also observed at the inlet bottom, as well as a vertically stratified velocity distribution.

Based on reseach results (Pan *et al.*, 2024), the inflow in this configuration shows similarities to a flat-plate boundary layer and can be classified as total pressure distortion. The low-momentum region remains concentrated in the lower half of the fan inlet, combining circumferential and radial features. Additionally, under cruise conditions, the airframe boundary layer remains nearly unchanged, so that the distortion can be considered steady over time. Representative aircrafts of this configuration includes D8 and ONEVA concepts.

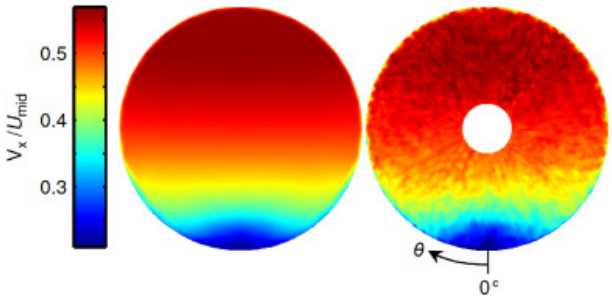

Figure 8 – Velocity distribution in fuselage mounted BLI fan configuration (Ma; Lu; Li, 2025)

2.2.3 Embedded Fans with S-Shaped Inlet Ducts

Lastly, another widely applied configuration BLI consists on an embedded fan with an S-shaped inlet duct. This configuration, although it has great advantages such as reducing drag and enhancing stealth performance of the aircraft, it also introduces a non-uniform pressure distribution, swirl distortions and flow separation. The boundary layer develops streamwise continuously along the duct, giving rise to a velocity deficit at the outlet which, together with the flow separation that occurs at the fan inlet due to adverse pressure gradients, causes a large loss of total pressure. This low pressure, causes higher levels of fatigue which decrease the service life of the engine.

Another characteristic feature of S-shaped inlet ducts is the paired swirl formed after the second bend. This phenomenon can be explained in two different ways (Guo; Seddon, 1982), based on considerations of pressure gradient and momentum or form a vorticity perspective. From the vorticity point of view, this vortex pair occurs when a flow with existing vortices is rotated in a direction perpendicular to its vortex vector. As the boundary layer flow within the duct is turned by the bend it generates two opposing vortices on each side of the duct exit, causing the flow to rotate in opposite directions toward its centerline.

The paired swirl formation can also be explained throught the pressure gradient and momentum. In a curved duct, pressure increases along the outer wall and decreases along the inner one, causing the high-velocity fluid in the core to be pushed towards the outer wall. Simultaneously, given that the low-energy fluid near the walls cannot overcome this pressure gradient, it is forced to move towards the low-pressure region on the inner wall. The combined movement of the high velocity flow deflecting outward and the low velocity flow moving inward creates two vortices within de duct. This inherent distorted flow pattern within the S-shaped inlet duct significantly impacts the aerodynamic performance of downstream fans/compressors.

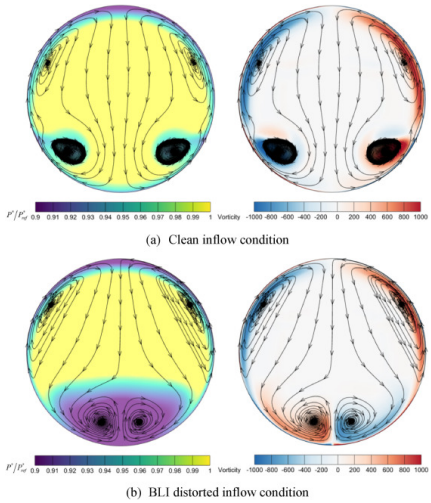

Figure 9 – Flow field at the outlet of an S-shaped configuration for clean inflow and BLI distorted inflow conditions

Overall, BLI configurations span from axisymmetric concepts such as the PFC, to fuselage-mounted fans and S-duct propulsors. More recent studies, extend BLI to advanced airfam architectures such as BWB, where a fully embedded distributed propulsion system is used(ref full thesis). These approaches underline how BLI is increasingly regarded as a propulsion integration strategy.

2.3 Reported Benefits of BLI Integration

Advances in BLI technology research have demonstrated, both conceptually and experimentally, that these types of propulsion systems offer multiple performance benefits. These advantadges mainly arise from the recovery of low-momentum flow in the aircraft wake, which reduces the aerodynamic drag and energy dissipation in the jet. As a consequence, measurable gains in the engine performance are obtained.

BLI propulsion systems take advantage of the low-momentum flow in the fuselage wake, which originates from viscous and form drag and represents a significant portion (55-65%) of the total drag on transport aircraft (Seitz A., 2015). Because this low-energy wake is ingested by the engine in these configurations, the downstream flow interacts with both the airframe and the propulsion system, contributing to both thrust and drag. Therefore, it is more appropriate to use momentum and energy conservation principles when sizing the engine (Hall *et al.*, 2017).

This interaction also provides a direct mechanism for improving propulsive efficiency, since the ingestion of low-momentum flow reduces ram drag (Sanders, 2018). This effect can be explained by assuming a propulsor with a perfectly expanded exhaust, whose thrust can be approximated as the amount of momentum transferred to the ingested flow,

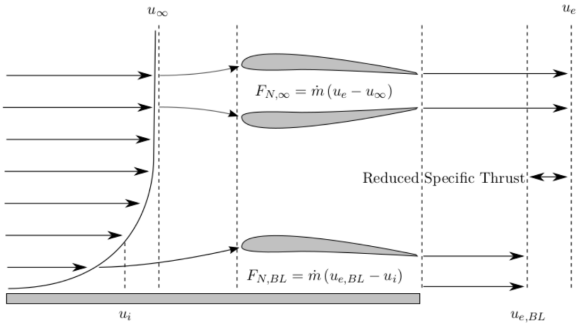

Figure 10 – Reduced Ram Drag effect on propulsive efficiency (Sanders, 2018)

$$\mathrm{F} = \dot{m}(u_e - u_i), \tag{2.2}$$

which assumes that the net thrust and intrinsic net thrust are equal. If its considered that the propulsor produces the same thrust for a given ingested mass flow rate, the difference between the inlet and exit flow velocity should also remain constant:

$$u_e = u_i + \Delta u = u_i + constant, \tag{2.3}$$

Additionally, the power required to generate thrust can be represented as the rate of kinetic energy transferred to the ingested flow, which, combined with the previous assumption, yields the following expression:

$$P = \frac{\dot{m}}{2}(u_e^2 - u_i^2) = \frac{\dot{m}}{2}\Delta u(\Delta u + 2u_i) \tag{2.4}$$

By analyzing the equation, it can be observed that as inlet velocity u_i increases, the power required to produce the same amount of thrust is also higher. Therefore, for podded engines, that ingest a free stream velocity airflow, it woud be necessary to reduce flight speed in order to obtain a power reduction benefit. However, the efficacy by which this power is transferred to useful propulsive work, becomes more evident at higher flight speeds, as illustrated by the definitions of propulsive efficiency, which expresses the ratio of propulsive power (product of thrust and airspeed) to the rate of kinetic energy imparted to the flow:

$$\eta_p = \frac{\dot{m}\Delta u u_\infty}{\frac{\dot{m}}{2}\Delta u(\Delta u + 2u_i)} = \frac{2}{(\frac{\Delta u}{u_\infty} + 2\frac{u_i}{u_\infty})} \tag{2.5}$$

Which in the case of podded installations have the form of:

$$\eta_p = \frac{2}{(\frac{\Delta u}{u_\infty} + 2)} \tag{2.6}$$

Although for both cases is clearly shown that the propulsive efficiency improves for higher flight airspeed, when comparing podded engines with BLI propulsive systems, it becomes evident that it improves for intake velocities lower than u_∞. Given that the airframe's BL is a possible way of reducing flow velocity for ingestion, the propulsive efficiency may be improved form BLI systems even at high flight speeds. Therefore, boundary layer ingestion leads to a decrease in the mechanical power needed to obtain a given thrust and hence, a reduction in fuel burn.

As a conclusion, even though the above descripiton does not fully account for all the true implications of BLI, it illustrates how this mechanism reduces ram drag and may improve the propulsion efficiency.

Another perspective that explains the BLI benefit arises from the minimization of kinetic energy losses in the wake with respect to free stream conditions. By analyzing the stream-wise velocity profile of wakes trailing behind free-stream and BLI configurations, it can be seen that the jet velocity profiles deviate positively while the profile behind airframe wakes deviate negatively, roughly cancelling one another out allowing a steady level flight. However, in the case of boundary layer ingesting configurations, the deviation is smaller due to the re-energization of the airframe boundary layers and thus, less energy is imparted to the atmosphere. Therefore, the aircraft's overall efficiency is improved by minimising its disturbance on the atmosphere.

This physical picture can be systematically formalized through the Power Balance Method, which shifts the performance evaluation from the momentum point of view to a power-based framework. By applying energy conservation, PBM enables a clearer accounting of losses and quantifies how much of the incoming power flow is effectively used to propel the aircraft. This energy-based method allows a decomposition of power sources and sinks across the flow field providing a better inside of how different mechanisms contribute to overall efficiency.

In addition to its improved efficiency, the BLI configuration offer other key benefits. The lower jet velocity required for the same thrust results in a reduction of noise (Liu *et al.*, 2022). Furthermore, the reduced SFC directly leads to lower emissions of carbon oxides and nitrogen oxides.

The theoretical benefits of BLI have been substained by experimental assesments of advanced aircraft concepts. A key example is the D8 double-bubble aircraft. Experimental evaluations of 1:11 scale model at the NASA Langley subsonic wind tunnel indicated power savings of 6% to 8% at cruise conditions (Uranga *et al.*, 2017). These results, obtained through a comparison with a non-BLI configuration, validated the performance gains from ingesting low momentum boundary layer flow. The use of the PBM in these studies allowed the low speed wind tunnel data to be scaled to full flight Reynolds numbers, confirming the relevance of the findings. More recent investigations focused on PFC (CENTERLINE

project) also demonstrated power savings of approximately 5% for an ideal BLI propulsor. These examples collectively provide experimental evidence that BLI is a viable technology for improving efficiency.

2.4 Challenges and Technical Limitations

Although current research has shown that boundary layer ingestion offers a promising path toward greater efficiency, it also adds new challenges that threaten the stable operation of the fan. Unlike conventional engines, which ingest free-stream airflow, BLI propulsors operate in a distorted flow field that compromise the aerodynamic and structural operation of the fan.

This distortion occurs mainly as a consequence of swirling flow and pressure and velocity variation imposed by the boundary layer. Furthermore, it is strongly dependant on the propulsor configuration and the boundary layer thickness (δ). For concepts in which the propulsor receives a nearly axisymmetric BL, this problem can be managed by designing the rotor blades with an angle that meets the radially varying velocities at a design point (Pardo; Hall, 2021b). However, for non axisymmetric inflows, the distortions cause a varying load on the fan blades as the rotate. Additionally, the complexity of its design its even more higher when accounting for the fact that the boundary layer thickness also varies with aircraft manouvers, which shifts the ingested distortion.

In order to provide an insight of how the fluid re-distributes through the fan numerous CFD studies have been conducted. In (Wang *et al.*, 2024), comparisons are made for different speeds and for increased circumferential distortions. A common way to define the circumferential distortion level is by using a distortion index such as DC60 which normalizes the dynamic pressure in front of the fan rotor and is defined as:

$$DC60 = \frac{\tilde{P}_{t,2} - \tilde{P}_{t60,min}}{\tilde{P}_{t,2} - \bar{P}_2} \tag{2.7}$$

In which $\tilde{P}_{t,2}$ denotes the average total pressure at the inlet and $\tilde{P}_{t60,min}$ the 60^{o} sector which corresponds to the lowest average total pressure.

The distortion levels indicated by this index is not merely a theoretical metric, they translate into real degradations in the performance and stability of the system. The boundary layer developed along the fuselage gaves place to a total pressure gradient at the fan inlet that significantly affects it aerodynamic efficiency and reduces its stability margin against compressor stall. As shown in (H.; F., 2024), the fan loses efficiency depending on the level and extent of the inlet circumferential distortion. This loss is due to the fact that the non-uniform flow forces each fan blade to operate under a varying aerodynamic load during every revolution. The load variatons can cause fatigue and reduced performance and also complicate the design, as the BLI fan must be able to tolerate constant distortion

unlike conventional engines exposed to clean inflow. Furthermore, this distortion is later transferred through the fan, affecting the performance of other engine components. As an addition, these distortion levels give rise to engine noise, which is one of the problems actually being addressed.

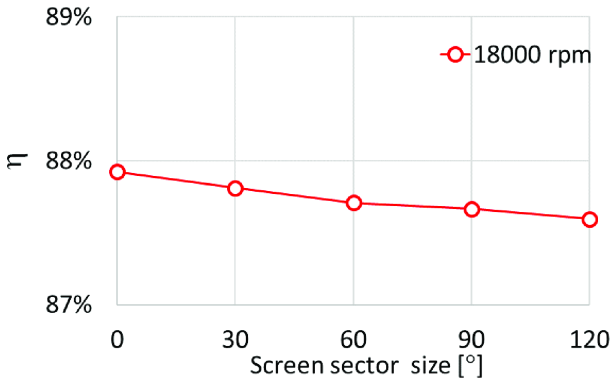

Figure 11 – (a) Sector Size vs. Propulsive Efficiency (H.; F., 2024)

The figure above shows how the propulsive efficiency η_p decreases as the angular size of the distortion region at the fan inlet increases.

The severity and type of distortion the fan experiences is also influenced by the design of the air intake. The research study (Wang *et al.*, 2024) analyzed S-shaped inlet ducts, a common concept used in BWB and fuselage integrated configurations that are particularly problematic. The curved geometry of these inlet ducts not only amplifies distortion but also introduces vortices and swirling flow in the air before it reaches the fan. In this way, the flow loses energy as it travels through the duct leading to a region of low total pressure. To understand this, CFD simulations were done showing a pair of vortices of maximum swirl angle of 23º at this low pressure region, which add considerable complexity to the design challenge of achieveing stability.

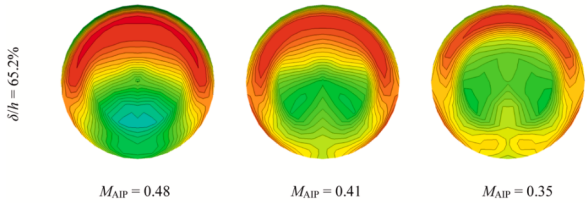

Figure 12 – Total pressure recovery coefficient for different Exit Mach Number (M_{AP})(Wang *et al.*, 2024)

In figure above, the higher pressure losses are shown in blue/green, while the better pressure recoveries are shown in red/orange. Therefore, this results show how the boundary layer ingestion leads to a total pressure loss at the fan inlet. Additionally, the countours of

the figure bellow show the intensity distribution of swirl in the fan inlet of an S-shaped configuration:

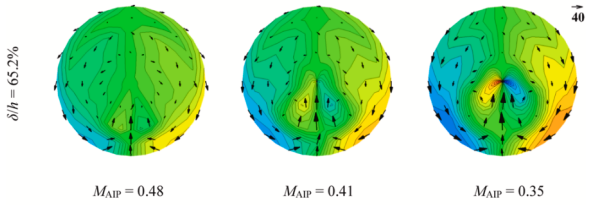

Figure 13 – Vortex formation for different Exit Mach Number (M_{AP}) (Wang *et al.*, 2024)

In order to understand the maginuted of these challenges, sub scale models such as the D8 "double-bubble" have been used to obtain experimental measurements and carry out CFD simulation of the tail-mounted configuration (Hall *et al.*, 2022). For this aircraft at its design point, measurements indicated 12% of distortion. However, under cruise conditions, the DC60 index showed more notable values in a range between 39% and 44%, reaching a maximum value of 62%. These high values highlight the importance of the problem and the need to develop propulsion technologies that are able to tolerate and minimize distortion.

Condition	α	$\Omega r_{tip}/V_\infty$	DC(60) (L)	DC(60) (R)
High α, idle	8 deg	1.28	0.437	0.617
Increased α	6 deg	2.71	0.442	0.479
Cruise	2 deg	2.70	0.390	0.442
High α	8 deg	2.71	0.342	0.454
Top of climb	2 deg	3.30	0.281	0.310
Start of climb	8 deg	5.70	0.132	0.142

Figure 14 – Measured DC60 for various simulated D8 mission operating conditions (Hall *et al.*, 2022)

3 METHODOLOGY

As stated previously, the objective of this work is to analyse the influence of boundary layer ingestion on turbofan performance. In order to do this, simulations were carried out using ANSYS ICEM CFD, in which the fuselage boundary layer was reproduced by introducing artificial disturbances on the wind tunnel walls, which allows analyzing how the ingested flow affects different parameters at the fan inlet. This section presents the details of the numerical model used and the different configurations tested, and explains the different steps followed in the numerical setup to obtain the results.

3.1 Experimental Design and Simulation Geometry

The simulations of this work are based on the EESC-USP Fan Rig configuration, which is a long duct with a low speed fan rig by DLR's test facility. The duct is approximately 10 meter long, and has a diameter of 0.6 m at the inlet and the outlet with a contraction to 0.5 m at the fan-stator stage, which was done with the purpose of reducing the casing boundary layer. To provide a smooth, axisymmetric inflow and reduce flow non-uniformities, an elliptical glass-fiber bell-mouth is installed at the inlet, while the outlet includes an anechoic termination that helps to minimize acoustic reflections.

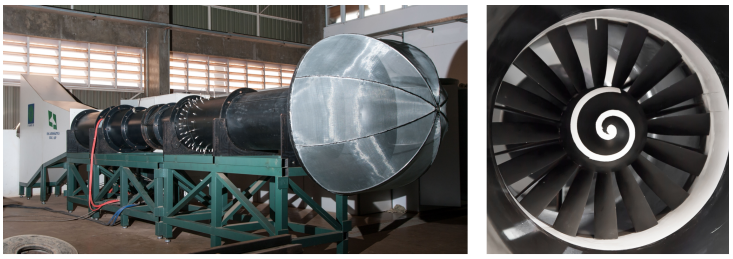

Figure 15 – EESC-USP Fan Rig configuration (Júnior *et al.*, 2017)

The fan's geometry is aimed to reproduce the NASA'S ANCF design. It consist of a 16-bladed rotor and a 14-vaned stator, and has a diameter of 0.5 m. This fan is drivem by a 100 hp Remy HVH-250-115 DOM electrical motors installed inside the duct, which is capable of reaching rotaional speed up to 4500 rpm, generating axial flows up to Mach 0.14 and tip speeds around 0.37. The Reynolds number relative to the rotor tip chord and speed is aproximately 400,000.

It should be noted that the proximity of the duct to the ground and the resulting flow asymmetries and turbulence differ from conditions encountered at the typical flight altitudes. Thus, the combination of these factors with ICD, influence the ingested flow and are considered in the analysis of the the boundary layer ingestion effects on fan performance (Júnior *et al.*, 2017).

When performing simulations in this wind tunnel under standard conditions, it can be observed that the only boundary layer present corresponds to that generated on the walls of the duct, which is too thin to significantly affect the fan. Therefore, to enable a representative analysis of BLI, artifical surface irregularities were introduced upstream of the fan section to reproduce the boundary layer within the CFD domain. For this purpose, a set of obstacles named as tooth was introuduced on the duct wall to generate turbulence and increase boundary layer thickness. As a result, a controlled low-momentum region is formed at the fan inlet, enabling the study of the impact of BLI on the engine performance.

In this context, a scale CFD domain mathing the geometry of the EESC-USP wind tunnel was developed. With this model, several simulations were carry out varing the tooth's shape and distance to the fan. All of these experiments were carried out following the same procedure.

3.2 CFD simulations

Before proceeding to study the effects of the boundary layer on the turbofan, it was necessary to analyze the effects that different tooth configurations have on the airflow entering the wind tunnel. This enables to determine which of these geometries most accurately reproduces the turbulence generated in reality along an aircraft's fuselage, which are ingested by these embedded engines.

To perform these simulations, an initial model of the wind tunnel without teeth was provided, which can be modified to include different tooth configurations and evaluate their effectiveness. In this way, the procedure for obtaining the final results includes the following steps:

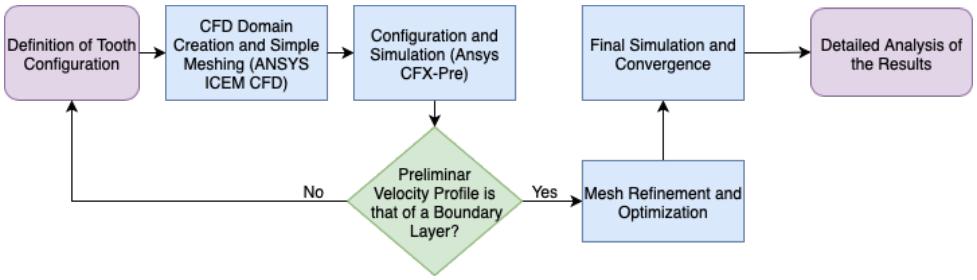

Figure 16 – Methodology for the Boundary layer Generation

3.2.1 Definition of Tooth Configuration

In order to determine which tooth configuration produces the most accurate and realistic boundary layer, three diferent geometries were proposed. These 'tooth' geometries were developed in CATIA and made available as *.step* files for integration into the simulation domain. The first configuration proposed is depicted in the figure bellow:

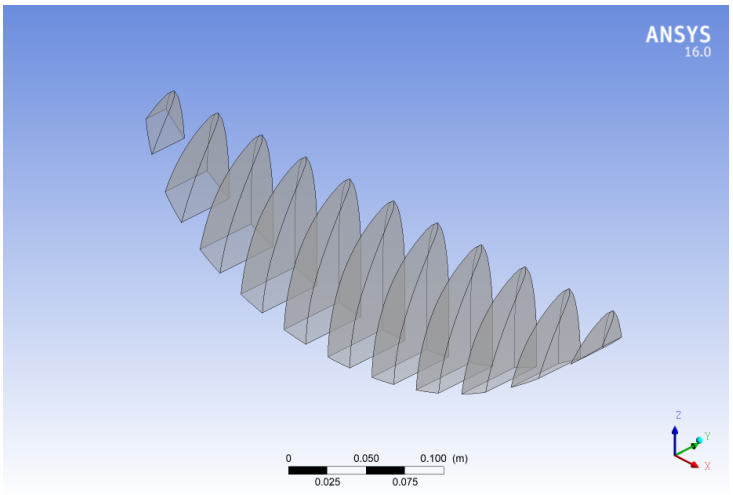

Figure 17 – Geometry 1: Base Tooth

This geometry was chosen as an initial approach to generate the desired boundary layer. Unlike a solid blockage that would completely obstruct the flow, this design was selected in order to introduce a controlled disturbance without compromising the overall properties of the incoming airflow. While a solid obstruction might seem to guarantee a uniform boundary layer, it would also cause significant flow separations and an excessive pressure drop that would drastically alter the fan inlet conditions. Therefore, this tooth geometry provides a balance between inducing the necessary turbulence to thicken the boundary layer while preserving the main flow characteristics.

However, an analysis of the lateral profile of this initial geometry, reveals that the upper section has a sharper edge that transitions to a more squared profile in the middle of the tooth. This abrupt change in geometry could introduce discontinuities in the boundary layer, leading to an irregular shape that would not accurately represent real conditions.

As a solution, a second configuration was analyzed, as shown in the figure below. This design replaces the previous profile with a uniform and oval shape. Thus, the objective of this revised geometry is to promote a smoother flow transition that would generate a more stable and representative boundary layer for the fan ingestion analysis.

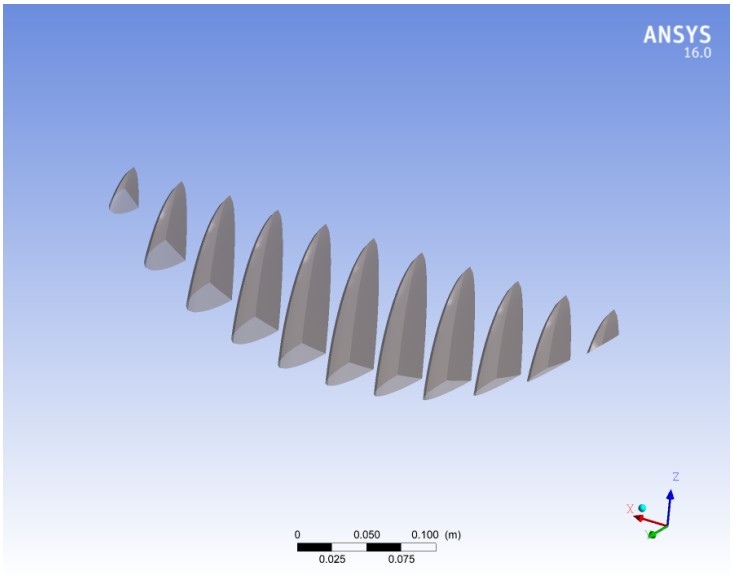

Figure 18 – Geometry 2: Oval Tooth

Finally, a third configuration was analyzed, the geometry of which is based on a more aerodynamic profile. This design, characterized by a thinner profile and a sharp leading edge, was investigated to study the influence of an even smoother flow transition. The shape was chosen to redistribute the area, thus preventing excessive momentum loss in the inner region of the BL and insufficient loss in the outer section.

A low wedge angle was selected, since it was expected to produce a vertical distribution of vorticity rather than a concentrated vortex. This angle was also mantained constant across all sections of the tooth in order to produce uniform turbulence and vorticity over its entire height (Counihan, 1968).

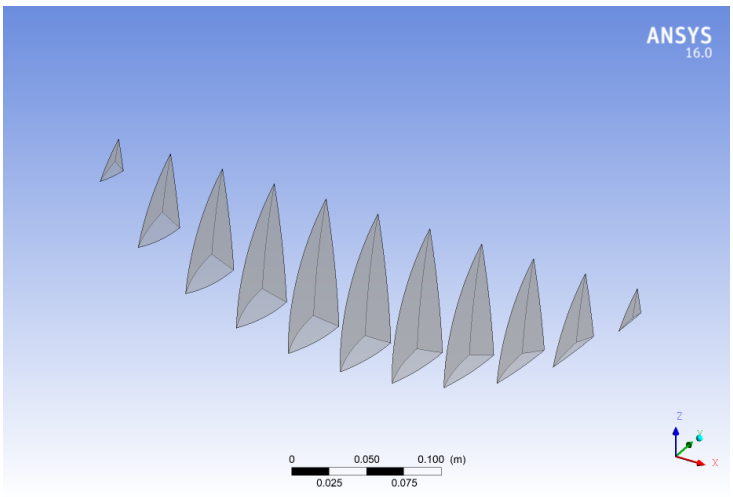

Figure 19 – Geometry 3: Sharp Tooth

Another aspect to be discussed when defining the tooth configuration is its height. This dimension is normally selected depending on the desired boundary layer thickness.

In this way, the design choice should take into account that this BL should be thick enough to significantly impact the fan performance without being too large to affect the characteristics of the free stream flow. Therefore, considering this reasoning and based on the experimental assesments in (Counihan, 1968) a height of approximately 0.1 m was chosen, which represents approximately 1/6 of the duct's diameter.

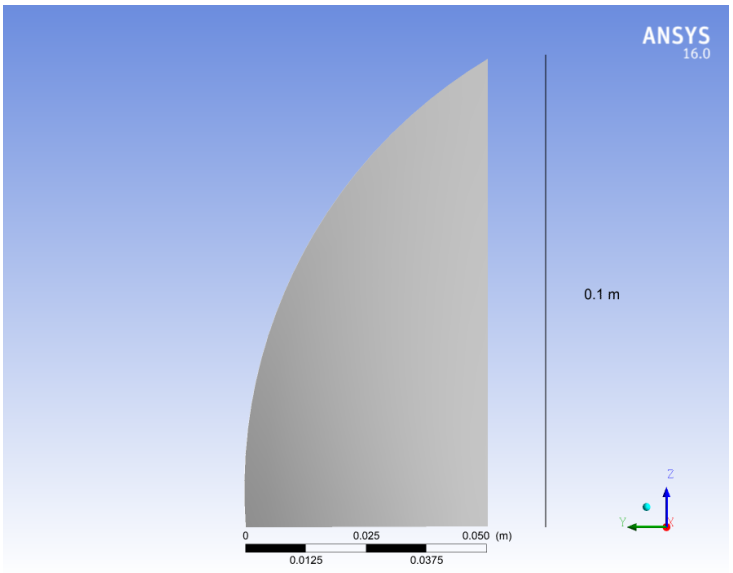

Figure 20 – Tooth height dimension

The lateral spacing between the obstacles was also a critical design parameter. It was considered that it should be as wide as possible, since as if they are installed too close the spacing might have some effect on the spectra of the turbulence.

3.2.2 CFD Domain Creation and Simple Meshing

The CFD simulations began with the preparation of the computational domain in ANSYS ICEM CFD, a pre-processing software tool for advanced geometry and mesh preparation. Each tooth configuration mentioned above was imported as a .stp file in order to integrate it on the intake of the wind tunnel. Although the intake's geometry was already provided as a CFD file, changes needed to be done to accurately include the obstacles on the duct. It should be noted that, since the changes are done only on the intake part of the wind tunnel, only this mesh shoukd be changed.

The CFD simulations began with the preparation of the computational domain in ANSYS ICEM CFD, a pre-processing software tool for advanced geometry and mesh generation. Each tooth configuration was imported as a .stp file to be integrated into the wind tunnel intake. Although the intake's geometry was provided as a CFD file, specific modifications were required to accurately include the obstacles.

An important aspect to consider when defining the geometry is the position and orientation of the tooth. Regarding orientation, the most aerodynamic part was positioned

as the leading edge, while the flat surface was designated as the trailing edge. This was done to ensure a smoother transition of the free stream flow, minimizing unnecessary flow disturbances. With respect to position, all configurations were placed at an arbitrary distance from the fan in such a way that a turbulent flow with the characteristics of a real boundary layer would reach it.

With the geometry correctly defined and prepared, a simple mesh was created for each configuration. This initial meshing strategy allowed for a rapid assesment of how effectively each design produced a consistent boundary layer. In this way, the generated meshes look as the following:

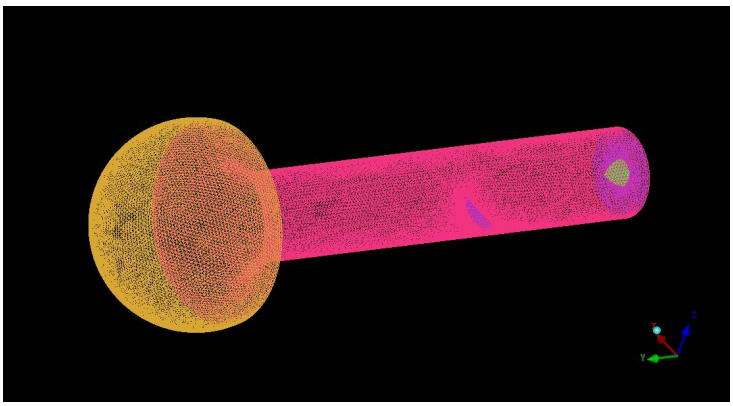

Figure 21 – Simple Initial Meshes

The mesh shown in the figure is a non-structured mesh, comprised of triangular elements on the surface and tetrahedral elements in the volume. This low density mesh, instead of providing high fidelity results, enables a more efficient design selection process with a reduced computational cost before moving on to a more refined mesh for the final analysis.

3.2.3 Configuration and simulation

Once the computational meshes were generated in Ansys ICEM CFD, they were imported into Ansys CFX-Pre. When imported, the software automatically reorganized the geometries of the wind tunnel intake, placing the tooth configurations in their correct positions and orientations. The process of setting up and running simulation was carried out in CFX-Pre. This section details the physical models and the numerical setups used to obtain the results.

The simulation of boundary layer ingestion in the turbofan necessarily involves the appearance of turbulent flow. Turbulence modeling is one of the main sources of uncertainty in CFD simulation. To address this Ansys CFX uses the concept of Reynolds-Averaged Navier-Stokes (RANS) equations.

Unlike DNS, these equations resolve turbulence structures by first averaging the conservation equations and then solving directly from the time-mean variables. In this way, due to the introduction of assumptions and approximations, RANS models are prone to modeling errors.

In Reynolds formulation (Tannehill; Anderson; Pletcher, 1997), every flow quantity (f) is decomposed into a time averaged component ($\bar{f}$) and a fluctuating component (f'), where $f = \bar{f} + f'$. The time averaged value is defined as:

$$\bar{f} = \frac{1}{\Delta t}\int_{t_0}^{t_0+\Delta t} f dt \tag{3.1}$$

Where Δt must be finite and should be large compared to the period of the random fluctuation, but small relative to any slow variations in the unsteady mean flow. By using these time-averaged variables, RANS replaces flow variables by these terms plus fluctuating components (e.g $u = \bar{u} + u'$).

With this formulation, the continuity equation in the Reynolds form can be expressed as following:

$$\frac{\partial \bar{\rho}}{\partial t} + \frac{\partial}{\partial x_j}(\bar{\rho}\bar{u}_j + \bar{\rho'u_j}) = 0 \tag{3.2}$$

The complete Reynolds momentum equations (all three components) can be written as:

$$\frac{\partial}{\partial t}(\bar{\rho}\bar{u}_i + \bar{\rho'u'_i}) + \frac{\partial}{\partial x_j}(\bar{\rho}\bar{u}_i\bar{u}_j + \bar{u}_i\bar{\rho'u'_j}) = -\frac{\partial \bar{p}}{\partial x_i}(\bar{\tau}_{ij} - \bar{u}_j\bar{\rho'u'_i} - \bar{\rho}\bar{u'_iu'_j} - \bar{\rho'u'_iu'_j}) \tag{3.3}$$

where

$$\bar{\tau}_{ij} = \mu[(\frac{\partial \bar{u}_i}{\partial x_j} + \frac{\partial \bar{u}_j}{\partial x_i}) - \frac{2}{3}\delta_{ij}\frac{\partial \bar{u}_k}{\partial x_k}] \tag{3.4}$$

Lastly, the third equation that RANS models use is the time-averaged Reynolds energy equations:

$$\frac{\partial}{\partial t}(c_p\bar{\rho}\bar{T} + c_p\bar{\rho'T'}) + \frac{\partial}{\partial x_j}(\bar{\rho}c_p\bar{T}\bar{u}_j + c_p\bar{T}\bar{\rho'u'_j}) = \frac{\partial \bar{p}}{\partial t} + \bar{u}_j\frac{\partial \bar{p}}{\partial x_j} + u'_j\frac{\bar{\partial}p'}{\partial x_j} + \frac{\partial}{\partial x_j}(k\frac{\partial \bar{T}}{\partial x_j} - \bar{u}_jc_p\bar{\rho'T'} - \bar{\rho}c_p\bar{T'u'_j} - c_p\bar{\rho'T'u'_j}) + \bar{\Phi} \tag{3.5}$$

where

$$\bar{\Phi} = \bar{\tau}_{ij} \frac{\partial \bar{u}_i}{\partial x_j} + \tau'_{ij} \frac{\bar{\partial} u'_i}{\partial x_j} \tag{3.6}$$

However, even though the RANS formulation eliminates the turbulence-related physics from the equations, turbulence models are required to close the problem and allow physically correct simulations. This is because the averaging process introduces new unknown termis, which must be modeled to solve the system of equations.

The turbulence model chosen for the initial simulations was the k-epsilon. This model was selected to provide an stable and quick first approximation of the flow characteristics for each configuration. However, during the analysis of the preliminary results, this model showed limitations in predicting the boundary layer. Therefore, for the definitive configuration, the k-epsilon model was replaced with the k-omega model, as it is specifically designed to handle boundary layer and the transition from laminar to turbulent flow with greater precision (Menter; Lechner; Matyushenko, 2021).

By combining the RANS formulation with the turbulence models discussed, Ansys is able to provide consistent data that allows the analysis of the effects of the boundary layer on fan performance.

Before running the simulations, the initial conditions were configured. A reference pressure of 92390 Pa was set, reflecting the atmospheric conditions of the closed space where the wind tunnel is located. Additionally, since the ambient air surrounding the wind tunnel is initially in static conditions, a relative pressure of 0 Pa was considered. An ambient temperature of 15^{o}C was assumed for the entire domain.

In all simulations, it was observed that the program did not reach a converged solution with an error lower than the one set. Instead, the solver terminated the simulation when it reached the maximum number of iterations. This behaviour is mainly caused by the presence of turbulence and is consistent both for the average and maximum values.

However, by analyzing the plots for the key properties (Mach number, mass flow rate, etc.) it can be seen that, after a certain number of iterations, the values of these varianbles stabilized and remained constat. Therefore, the simulations were stopped at this point, since these results were considered representative of the final state.

3.2.4 Mesh Refinement and Optimization

The low density preliminary mesh helped to select the geometry with the best performance for producing an efficient boundary layer. However, in order to define it clearly and obtain reliable results, a higher quality mesh was required.

When observing the initial results, it was seen that the preliminary mesh failed to accurately characterize certain aspects of the boundary layer. In order to create a more

accurate mesh, it was necessary to consider not only the boundary layer generated by the tooth but also the natural BL developing along the duct wall. Although the latter is comparatively thinner, neglecting it could introduce unrealistic effects on the overall flow.

To adress this problem, the duct geometry was divided into three different sections and for each of them, a different structured mesh was generated. This enabled to control precisely the quality and size of the elements according to the physical phenomena of interest in each part. The three stablished sections were the parts upstream and downstream of the tooth and the cylindrical region containing the tooth:

3.2.4.1 Upstream of the tooth

This section, which refers to the area between the intake and the teeth, was meshed with the structure shown in the figure bellow:

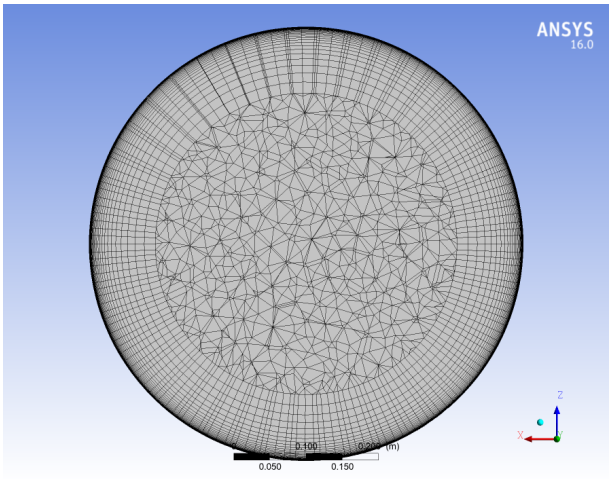

Figure 22 – Structured Mesh Upstream of the Tooth

Among the three meshes, this part has the least refinement, as the turbulence in this section is only due to the natural wall boundary layer. Additionally, given its distance from the fan, it does nos affect much on its performance.

Therefore, the only requirement for this mesh was that it needed to be refined enough along the height of the wall boundary layer in order to characterized it as accurately as possible. To achieve this, a stuctured prismatic mesh was created using the following parameter:

Parameter	Value
Growth Law	Exponential
Initial Height	0.0049999999 mm
Height Ratio	1.2
Number of Layers	45

Table 1 – Configuration parameters of the prismatic mesh of the upstream section of the tooth

These parameters resulted in a total structured mesh height of aprxomately 76.17 mm, which is more than sufficent to accurately and precisely characterize the boundary laver developing along the walls of the duct. This structured prismatic mesh is used only near the walls while the central area of the duct is filled with an unstructured mesh.

3.2.4.2 Region of the tooth

In the teeth region, creating a high quality computational mesh is more difficult due to the compplex geometry of the obstacles themselves. The pesence of these structures introduce significant challenges to meshing since the mesh quality in this zone must be very high in order to correctly characterize the flow around each tooth. However, this high level of refinement leads to substantial increase in the computational cost of the simulation. Therefore, the following mesh was generated for this part which balanced precision and efficiency:

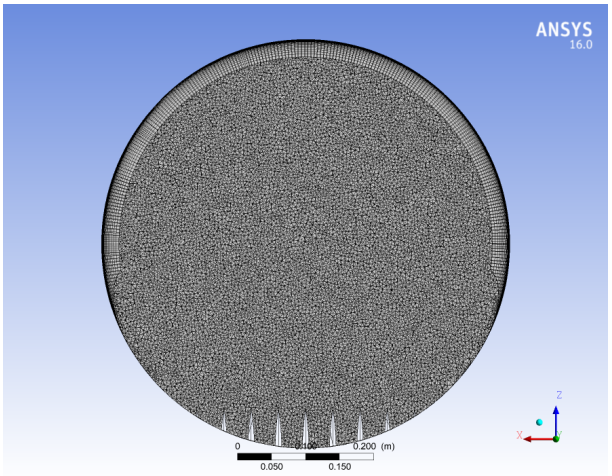

Figure 23 – Structured Mesh on the Tooth Region

As it can be seen in the figure, this section was divided into two halfs to generate a mesh as more precise as possible. At the bottom, where the teeth are located, a highly refined unstructured mesh was used to accurately capture the complex geometry of the obstacles. Meanwhile, on the top and side walls of the duct, a structured region of prisms was generated to properly characterize the boundary layer of the wall. In this case, the meshing parameters used to create this prismatic structured mesh were:

Parameter	Value
Growth Law	Exponential
Initial Height	0.0049999999 mm
Height Ratio	1.2
Number of Layers	38

Table 2 – Configuration parameters of the prismatic mesh of the tooth region

In this way, a prismatic mesh of approximately 21.24 mm was created only for the upper half of this region.

3.2.4.3 Downstream of the tooth

The section downstream of the tooth is the region of most interest since is where the boundary layer to be ingested by the fan develops. In order to characterize this boundary layer, a prismatic structured mesh was created in the near-wall regions. This mesh was designed with a greater high than in the previous sections, as the boundary layer generated by the tooth is significantly thicker than the wall BL.

Therefore, it was necessary for the structured mesh to extend further from the wall to fully capture the boundary layer. As stated before, this type of mesh is highly effective in defining the shape and properties of the boundary layer with precision.

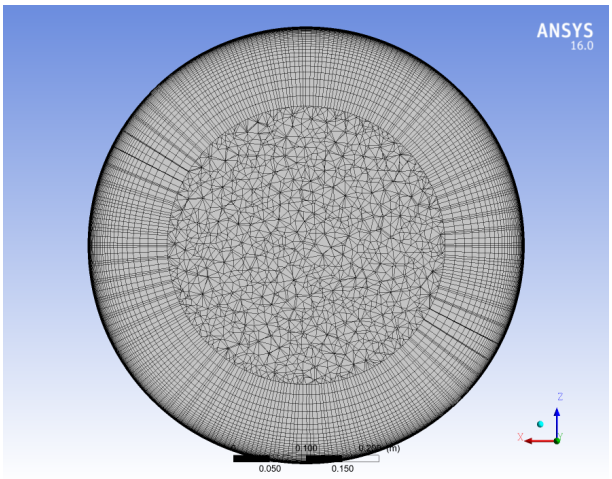

Figure 24 – Structured Mesh Downstream of the Tooth

The resulting mesh reached a total height of 109.12mm, a dimension large enought to accurately characterize the flow in the hole boundary layer region. The parameters used for this meshing were:

Parameter	**Value**
Growth Law	Exponential
Initial Height	0.02 mm
Height Ratio	1.15
Number of Layers	48

Table 3 – Configuration parameters of the prismatic mesh of the downstream section of the tooth

Once the definitive mesh was created, it was exported to Ansys CFX-Pre. The simulation was then run to obatin more precise and reliable results with this improved mesh. With these results, we could proceed with the analysis to determine how the boundary layer ingestion affects the fan's performance by comparing them with the results obtained from a clean simulation.

4 RESULTS

Before analyzing the effect of the boundary layer ingestion on the fan performance, a comparative analysis was performed on the different configurations to determine which one most accurately and precisely recreates the boundary layer. This evaluation used the results obtained from simulations in which the refined computational mesh defined in section 3.2.4 was used.

Once the configuration that yields a turbulent flow with a coherent behaviour was identified, its performance properties were then compared to those of an unobstructed wind tunnel.. This was done to quantify the effect of BLI and determine if these results could be extrapolated to real life to study real-world scenarios.

4.1 Comparison of Configurations

To evaluate the impact of each tooth configuration on the airflow, a comparative analysis of four main properties was performed. This included a qualitative assesment of the velocity profiles on both, a central longitudinal plane showing a side view of the wind tunnel and a cross sectional plane which shows the shape of the BL around the duct's circumference. Additionally, a quantitative analysis was performed on the evolution of both velocity and turbulent kinetic energy along the z direction. This approach was used to validate the simulation results against expected physical phenomena and to determine which configuration produced the most effective turbulent boundary layer.

4.1.1 Velocity Profile on a Central Longitudinal Plane

After running each simulation and obtaining the results, a longitudinal plane (YZ plane) was created, which cuts the entire wind tunnel through its center (x=0). A contour plot was then generated on this plane to visualize the velocity distribution across the entire domain and observe the shape of the boundary layer created by each configuration.

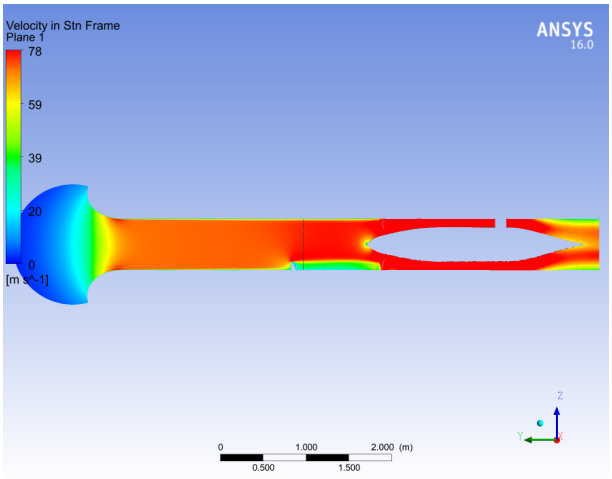

[b]

Figure 25 – Velocity contour plot on a longitudinal plane for the base tooth configuration

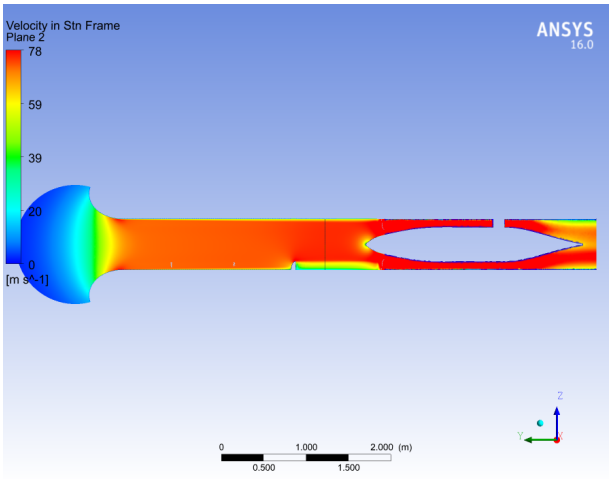

[b]

Figure 26 – Velocity contour plot on a longitudinal plane for the oval tooth configuration

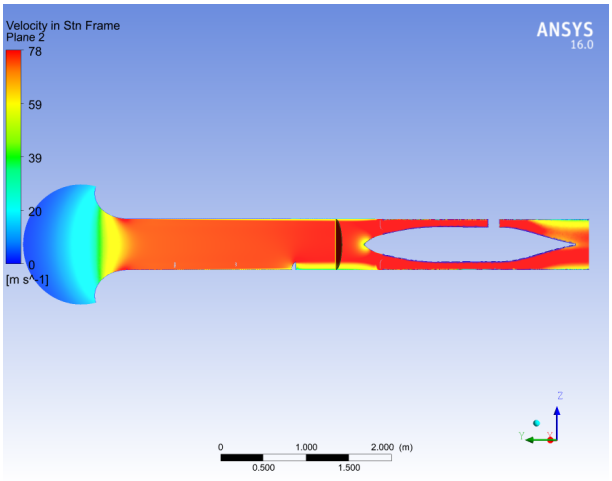

[b]

Figure 27 – Velocity contour plot on a longitudinal plane for the sharp tooth configuration

These velocity contour plots confirm that all three configurations successfully generate a region of reduced velocities behind them, which is consistent with the formation of a boundary layer. While these qualitative visualizations confirm the desired effect, they do not allow to determine precisely if the BL shape and properties are similar to a real case.

4.1.2 Velocity Profile on a Cross Sectional Plane

In order to determine whether the boundary layer generated by each geometry resemble those formed along the fuselage of an aircraft, a cross-sectional cut was done in the intake duct at a distance of 0.65 from the fan. This location was selected arbitrarly, as it was expected that at this point the boundary layer would have already uniformized, allowing for a clear analysis of its shape.

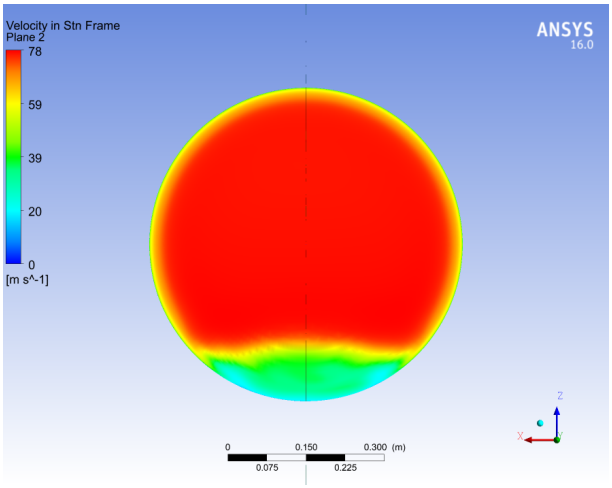

Figure 28 – Velocity contour plot on a cross-sectional plane for the base tooth configuration

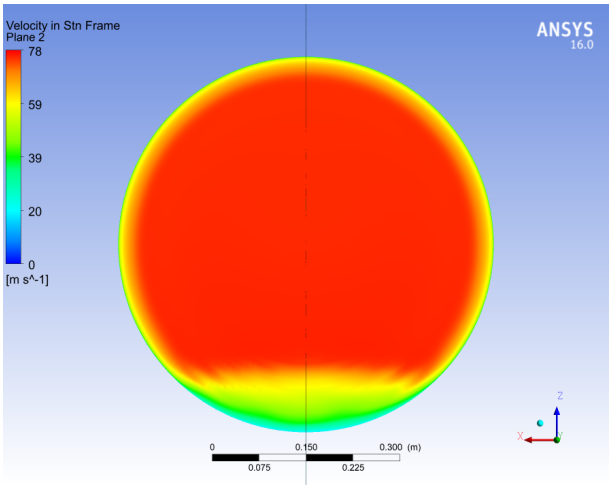

Figure 29 – Velocity contour plot on a cross-sectional plane for the oval tooth configuration

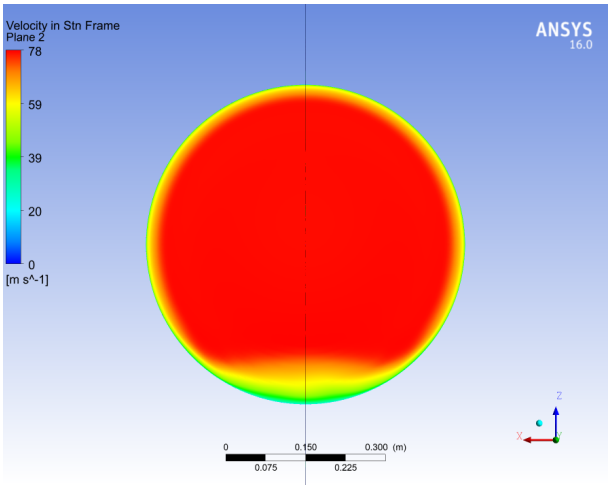

Figure 30 – Velocity contour plot on a cross-sectional plane for the sharp tooth configuration

The boundary layer was expected to be irregular only in the region very close to the teeth, quicky becoming uniform over a short distance. As it moves away from the tooth and approaches the fan, its shape should take on a more circular profile.

Analyzing the velocity profiles in this cross section, it can be observed that the base and oval configurations present non uniform sections, resulting in a less regular boundary layer that does accurately reproduce reality. The sharp configuration on the other hand, shows a more uniform and rounded distribution, suggesting that its BL more closely resembles the expected shapes.

As mentioned in the introduction, the objective is to reproduce the boundary layer that would be ingested by an engine integrated on the upper surface of a Blended Wing Body configuration. In such designs, the boundary layer upstream of the engine develops along a large, nearly flat surface, and therefore it can be reasonably approxiamated as planar with a rounded shape on the sides. For this reason, the sharp configuration is choses, as it provides a boundary layer profile that most closely resembles the planar ingestion expected in a BWB.

4.1.3 Velocity Distribution Along the Z-Axis

To analyze the evolution of velocity within the boundary layer, a line was created in the cross-sectional plane that spans the duct from the point (0,0.65,-0.3) to (0,0.65,0.3). This line was used to generate a plot in which the velocity values at each point along the z-axis were represented.

In all these graphs, the thickness of the duct's wall boundary layer is visible, which has a value of approximately 0.03 m. This can be observed by noting that the velocity in the upper part of the duct reaches a uniform value at this distance from the top wall.

In this way, the velocity profile for the base tooth configuration is shown in the following graph:

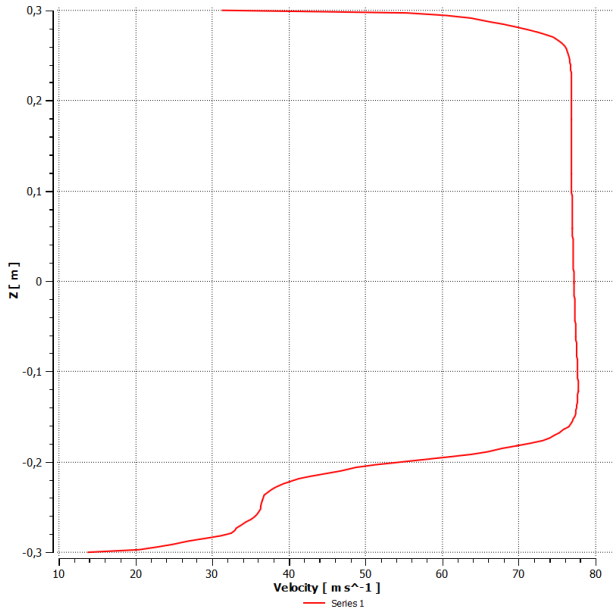

Figure 31 – Velocity distribution for the base tooth configuration

This graphs reveals that this configuration is not suitable, as the velocity in the boundary layer section shows a significant irregularity between z=-0.28 and z=-0.23. In this region, the velocity remains relatively constant instead of increasing smoothly and continuously as expected in a BL. When analyzing the geometry of the tooth, it was observed that the point of this irregularity coincides with the location where teh tooth's shape passes from being more rectangular to an oval profile.

Given the observed irregularity, a second configuration was designed with a continuous oval profile to avoid any abrupt changes in geometry and, thus in the velocity distribution. The velocity distribution for this oval configuration resulted to be the following:

Although this graph does not show the same sudden change in trend as the first configuration, the results are still not ideal. The velocity in the boundary layer, instead of increaing continuously and uniformly, presents irregularities and changes in slope that are not characteristic of a well-developed boundary layer. Therefore, based on the research in (Counihan, 1968), a third configuration with a more sharp geometry was designed which yielded the following results:

In this case, the velocity within the boundary layer increases continuosly and smoothly, without any sudden changes in trend or slope. Due to this behaviour, it was consider to effectively represent the evolution of velocity within a real boundary layer.

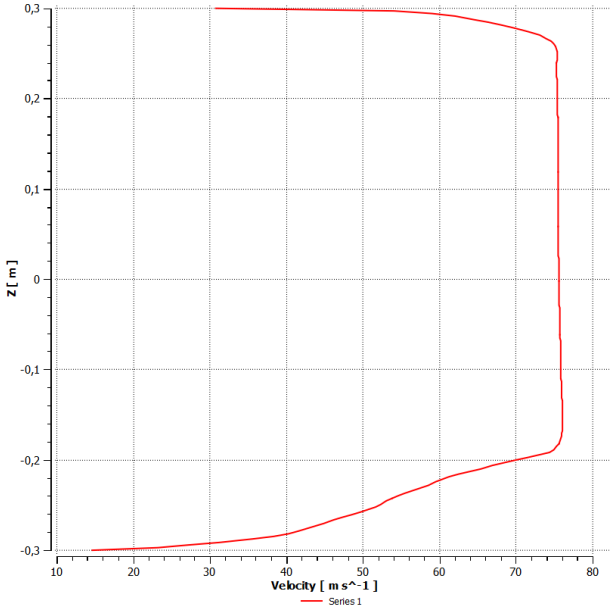

Figure 32 – Velocity distribution for the oval tooth configuration

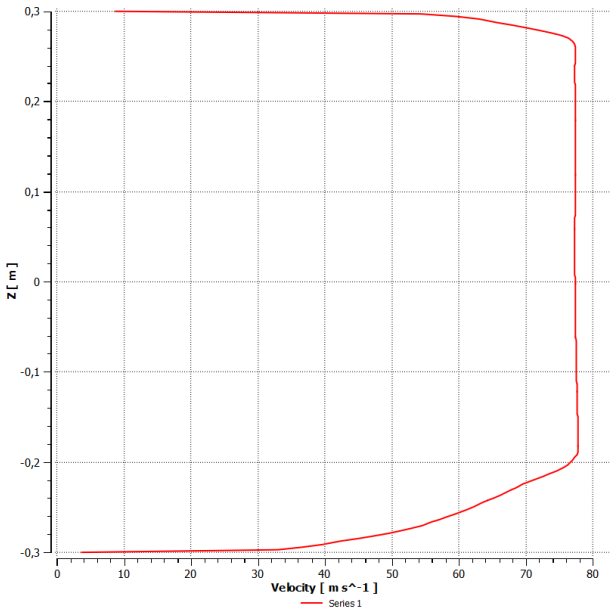

Figure 33 – Velocity distribution for the sharp tooth configuration

4.1.4 Turbulence Kinetic Energy Distribution

Another way to validate the properties of the induced boundary layer is by observing the turbulence kinetic energy distribution along the z-axis. In this way, the same line as in the velocity analysis was used to generate plots to study the evolution of this property. To consider the boundary layer correct, its TKE value near the wall should be significantly greater than zero near the walls and should decrease continuously to zero as the distance from the wall increasesm reaching this value in the free-stream flow region.

It is expected that TKE will be greater than zero in both the induced boundary

layer and the wall boundary layer. However, the value is expected to decrease more slowly and continuosly in the case of the BL generated by the tooth.

Additionally, it is important to note that in all the cases, the TKE should be higher in the duct walls that in the induced boundary layer. This is because the flow has a higher velocity in the upper part of the duct than in the lower part, where it is obstructed by the tooth.

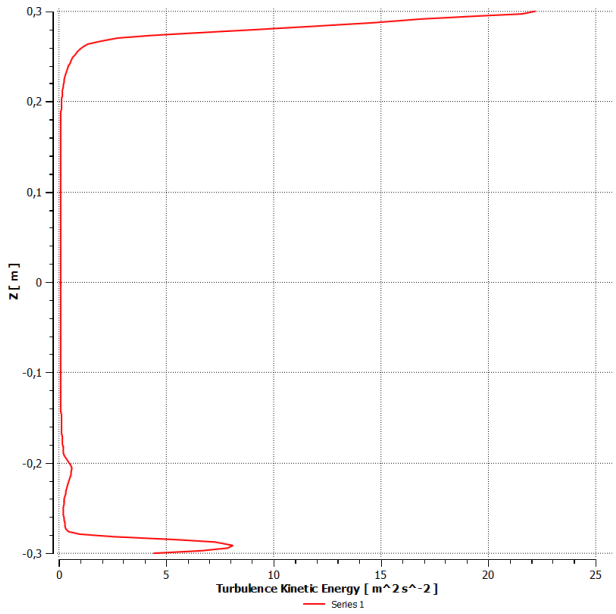

Figure 34 – TKE distribution for the base tooth configuration

The graph for the first configuration shows that it is not suitable for representing a real boundary layer. Although the TKE appears to approach zero appropiately, it shows an irregular increase in turbulence for higher z values.

In the case of the oval tooth configuration, irregularities similar to the first case can be observed in the lower boundary layer region. The TKE begins to decrease rapidly, but after reaching a low value, the curve's slope changes drastically, causing it to increase very slowly until it reaches zero.

Finally, for the sharp configuration, which has so far demonstrated logical boundary layer properties, no irregularities are present in the turbulence behaviour. In the lower part of the duct, where the induced boundary layer is located, the TKE reduces more slowly and continuosly than in the upper wall BL before reaching zero. The reason why this happens is that the induced boundary layer is thicker than the latter.

It should also be mentioned that the sudden reductions in turbulence for values very close to the wall are due to modeling errors caused by software limitations. In reality, the region nearest the wall is where the turbulence has its highest values. However, this error does not affect the analysis of the TKE distribution.

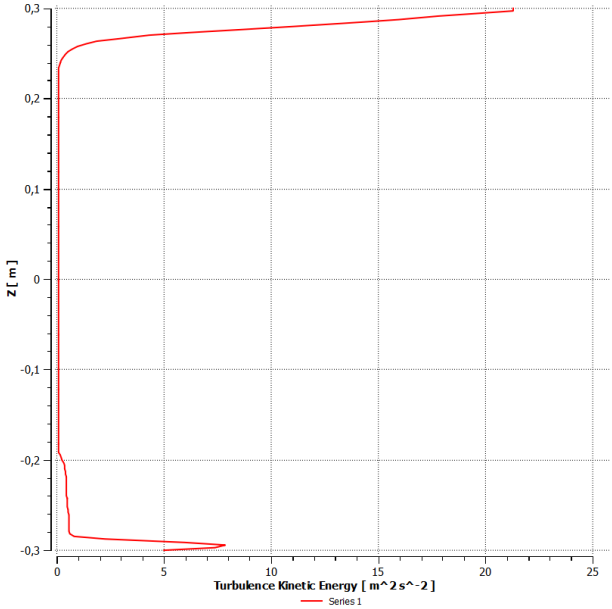

Figure 35 – TKE distribution for the oval tooth configuration

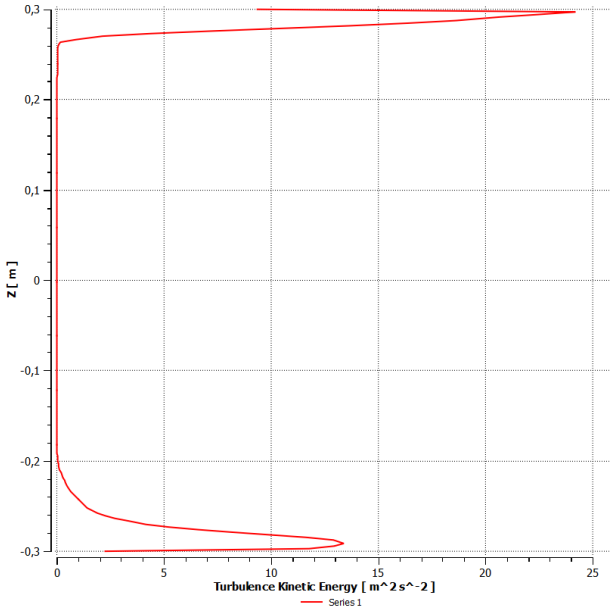

Figure 36 – TKE distribution for the sharp tooth configuration

Based on the analysis of these four parameters, the sharp configuration was determined to be the most suitable since these results are mantained in all its extension. Therefore, this configuration was used for further analysis to quantify the effects of BLI on the engine's performance and to see if these results could be extrapolated to practical applications.

4.2 Analysis of Results

Having established a method to generate a realistic boundary layer, the results of the simulation were then analyzed to quantify how it impacts on fan performance. To do this, parameters such as thrust, torque, propulsive efficiency, and the variation in both total and static pressure were obtained and compared to the results of a baseline simulation with no tooth. The latter simulation represents the fan operating under normal, unobstructed conditions. The analytical comparison of these two sets of values allows for a precise quantification of the BLI effects and reveal if this simulation accurately represents reality.

4.2.1 Thrust, Torque and Fan Efficiency

When discussing fan performance, the most relevant parameters to examine are the thrust it is able to generate and the torque required to produce that thrust value. With these two parameters it is possible to calculate the efficiency of the fan which serves as a key indicator of the efficiency with which the fan converts energy into useful power.

These values were easily obtained in both simulations by calculating the force and torque on the y-direction of the rotor blades using the Function Calculator in Ansys CFX-Post. The force was expected to have a positive value, as it acts as a reaction to the airflow which is being pushed in the opposite direction. On the other hand, given the rotor's counterclockwise rotation of the rotor, the torque was expected to have a negative sign reflecting the fluid's resistance to rotation. The results obtained for both simulations are represented in the table bellow:

Configuration	**Thrust (N)**	**Torque (N·m)**
BLI configuration	1044.72	-211.968
No teeth configuration	1032.05	-210.474

Table 4 – Comparison of thrust and torque for BLI and clean wind tunnel configurations

By comparing the results of the BLI configuration with those of the clean wind tunnel simulation, it can be clearly seen that the variatons in fan performance were minimal. It is shown that the BLI generates a small increase in thrust of approximately 13N, while it also requires a slightly higher torque (1.5 Nm more or less). In this way, this increase in thrust comes with a higher power demand. These variations could be more clearly understood by comparing the fan's efficiency for both cases:

$$\eta_{fan} = \frac{T \cdot V_{outlet}}{\omega \cdot \tau} \tag{4.1}$$

Where the outlet velocity (V_{outlet}) was 73.853 m/s for the BLI configuration and 73.9957 m/s for the clean case. The angular velocity (ω) remained constant at 471.239

rad/s in both simulations. With this expression, the fan efficiency obtained for each configuration was:

Configuration	**Fan's efficiency**
BLI configuration	0.7724
No teeth configuration	0.7700

Table 5 – Fan's efficiency for each configuration

A These results show a slightly higher efficiency for the obtructed configuration. This phenomenon is a direct result of the BLI itself, since, although both thrust and torque increased, thrust grew proportionally more than torque. This shows that this small increase in torque was efficiently leveraged to create a greater thrust.

However, the difference in efficiency between the two cases is minimal, of 0.0024, which is probably within the numerical margin of error for the simulations. Thus, it can be concluded that, although this sharp configuration generates succesfully a boundary layer with realistic characteristics, it does not show a representative effect on these performance parameters under the set conditions.

4.2.2 Total and Static Pressure Variations

Analyzing the pressure variation across the fan is also essential to study the energy transfer to the flow. The total pressure gain (ΔP_t) represents the total energy added to the system, while the static pressure variation (ΔP_s) reflects the aerodynamic forces acting on the fan. For this purpose, the total and static pressure gains and losses across the rotor and stator were calculated for both configurations. It should be noted that the values of P_s are taken relative to the specified ambient pressure. The results are shown in the following table:

Parameter	**BLI Configuration**	**Clean Configuration**
Total Pressure (ΔP_t)		
$\Delta P_{t,rotor}$	4692.252 Pa	4655.62 Pa
$\Delta P_{t,stator}$	-452.86 Pa	-457.85 Pa
ΔP_t	**4239.392 Pa**	**4197.77 Pa**
Static Pressure (ΔP_s)		
$\Delta P_{s,rotor}$	1778.66 Pa	1731.47 Pa
$\Delta P_{s,stator}$	-1355.92 Pa	-1395.43 Pa
ΔP_s	**422.74 Pa**	**336.04 Pa**

Table 6 – Comparison of total and static pressure values for both configurations.

When observing the results for total pressure, it is seen that the gain is slightly higher for the BLI configuration (4239.392 Pa) compared to the unobstructed configuration

(4197.77 Pa). This indicates that the BLI fan is transferring more energy to the flow overall, which is an interesting but not much representive result due to the small difference.

The contribution of the rotor to the pressure is also slightly higher in the BLI configuration, which suggest that the ingestion of the BLI affects positively the rotor's ability to perform work. In turn, the pressure loss across the stator is slightly lower in the BLI configuration than in the clean wind tunnel. This indicates that the presence of the boundary layer alters the flow in such a way that the stator blades operate a bit more efficiently.

The greater total and static pressure gain in the tooth configuration is consistent with the fact that it generated a slightly higher thrust. However, even though these BLI results showed an improved rotor performance and lower stator losses, the small pressure gains and the corresponding increase in torque did not translate in a representative increase in fan efficiency.

4.2.3 Pressure Distribution and Structural Analysis

The final part of the analysis is focused on the pressure distribution on the rotor blades. Unlike in a clean configuration, the BLI case showed a non-uniform pressure load on the blades, with higher values on the blades located in the lowest position (39.55 N) compared to the upper blades (35.24 N). This irregular loading is a very important aspect to consider when analyzing the BLI effects. Under working conditions, this continuous oscillation of pressure in working conditions, could lead to vibrations and fatigue issues over time compromising the structural integrity of the fan.

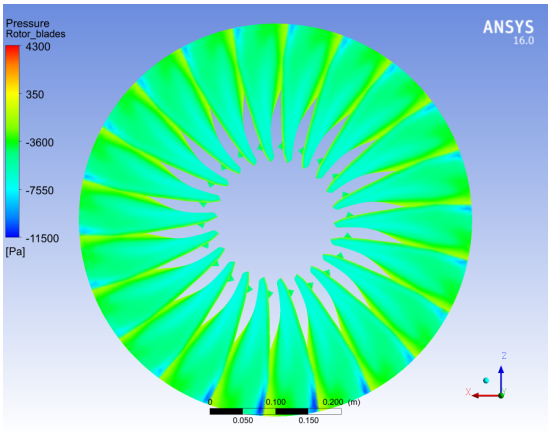

Figure 37 – (a)

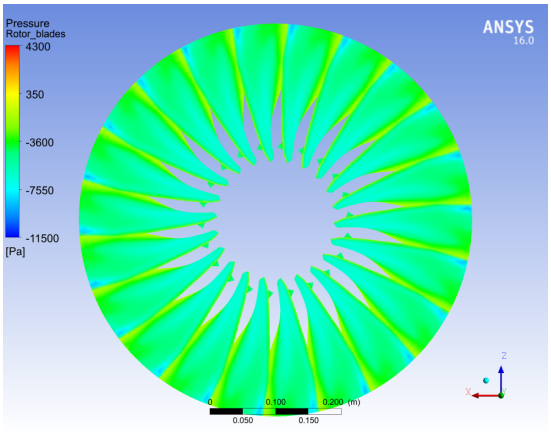

Figure 38 – (b)

Figure 39 – Pressure distribution on the rotor blade for (a) BLI configuration (b) Clean configuration)

However, in addition to these aerodynamic forces, the blades must withstand

centrifugal force, which are much larger in magnitude. As the simulation software cannot directly calculate these type of forces, an analytical method was employed for comparison. To do this, the mass (350g) and radius (300mm) of a single blade were measured, and the centrifugal force was then calculates using the following expression:

$$F_{centr} = m \cdot r \cdot \omega^2 \tag{4.2}$$

where ω refers to the rotational velocity (4500 rpm). For comparison, the aerodynamic force exerted by the flow and the moment in X and Z were calculated using the Function Calculator in Ansys CFX-Post to understand the relevance of these forces. The results are summarized in the table below:

Parameter	**Value**
F_{centr}	23316.95 N
$F_{aerodyn.}$	39.55 N
M_z	-1.0973 N m
M_x	30.6171 N m

Table 7 – Forces acting on the rotor blades

The results confirm that the aerodynamic force exerted by the flow is negligible when compared to the centrifugal forces, which are much larger. Therefore, although over time the asymmetrical application of aerodynamic forces could contribute to material degradation and fatigue, their effect will be minimal since the blades are designed to withstand the dominant centrifugal loads.

In order to have a more detailed view of this non-uniform pressure distributions, two polylines were created: one on the tip of the bottom blade (with higher loads) and another on the tip of the top blade (with lower loads). These polylines were positioned in locations with critical pressures values by using a temperature contour plot as a guide to ensure they followed the exact outer edge of the blades. With them, two different plots were generated to analyze how the pressure changes along the x-axis (which is the axis that better follows the blade geometry). For a clearer analysis, the Pressure Coefficient (C_p) was calculated and used for the plots. The following images show the evolution of this variable in the bottom blade:

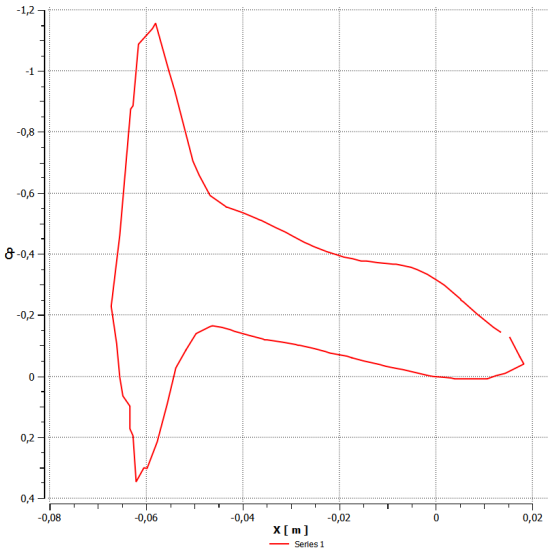

Figure 40 – C_p distribution along the polyline on the bottom blade

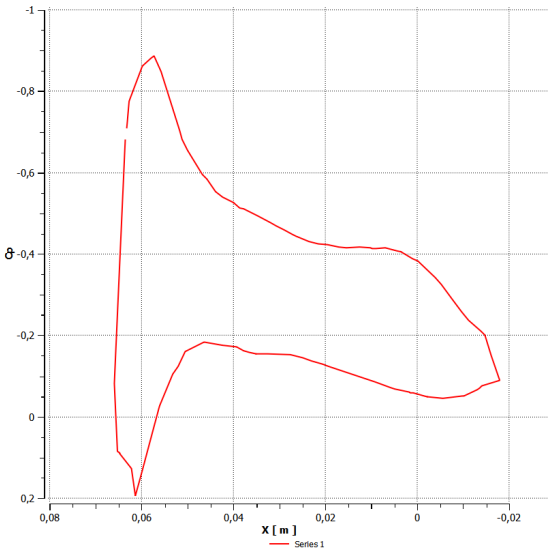

Figure 41 – C_p distribution along the polyline on the top blade

Figure 42 – Pressure Coefficient distribution along the tips of the bottom and top rotor blades in the BLI configurations

The C_p plot for the bottom blade provides a quantitative view of the high pressure distribution. The negative values on the upper curve represent the low-pressure side, which counts with intense suction. On the other hand, the lower curve shows the high pressure on the opposite side, the surface pushed by the airflow. The significant vertical separation between the peaks of these two curves indicates that this blade section is subjected to a high aerodynamic load which greatly contributes to thrust. In the case of the top blade, the separation between the suction and pressure sides is much smaller, indicating a lower pressure differential and thus, a lower aerodynamic load.

Therefore, it can be concluded that BLI creates a non-uniform velocity profile that causes a loading disparity across the fan, forcing the bottom blades to do more work. In contrast standard, clean configurations have uniform velocity profiles which result in equal loads in all blades.

5 CONCLUSIONS AN FUTURE WORK

Based on the numerous simulations conducted to obtain a well-defined boundary layer and analyze its effects on fan performance, this study has led to several important conclusions. This process involved first determining the most suitable configuration for generating boundary layer and then analyzing how various fan parameters responded to BLI.

5.1 Boundary Layer Generation

The determination of the most adequate obstacle configuration to generate a turbulent boundary layer with consistent properties was critical for the development of this study. After various geometry modifications and optimization iterations, it was proven that the implementation of a set of tooth-like geometries in the wind tunnel succesfully achieved the desired flow conditions.

The various simulations demonstrated the crucial importance of the geometry, orientation and position of the obstacle, since not all of the proposed configurations were capable of generating a realistic boundary layer. To be successful, the configuration needed to adapt the flow smoothly, allowing the generated turbulence to evolve and grow realistically as it approached the fan. Any geometric discontinuity, such an abrupt change in shape, led to irregularities in the velocity distribution that did not resemble a boundary layer profile.

This explains why the sharp tooth was the most suitable configuration among the proposed designs. This geometry brings together all the required characteristics. Its thin leading edge allows the flow to deviate smoothly, giving to turbulence gradually without sudden drastic magnitudes that could lead to further irregularities. The uniform contour shape of the tooth, prevents the geometry itself from creating different flow tendencies. Additionally, its low thickness ensures that a boundary layer is generated without compromising the properties of the rest of the incoming airflow, which is important for recreating accurately a real world case.

5.2 BLI Effects on Fan Performance

The analysis of various fan performance parameters shows that BLI provides some benefits while also introducing challenges. The results, although they show minimal changes compared to a clean configuration, reveal a clear trend that is consisten with previous research.

The propulsive efficiency of the fan, for example, showed a favorable trend. The thrust experienced an increase of 13N, while the required torque increased by only 1.5 Nm. This translated into a slight increase in propulsive efficiency of 0.0024. While this change is almost insignifican in magnitude, the proportional increase in thrust over torque suggest that under different conditions more similar to reality, this phenomenon could lead to a more representative efficiency increase. Similarly, the anlysis of static and total pressure variations also indicated minor but favorable gains for the BLI configuration, which translates into a greater energy addition to the fluid.

The main challenge highlighted by this simulation is an unequal load distribution on the rotor blades. As stated previously, the higher loads experienced in the lower part of the fan, could cause oscillations that affect the structural integrity of the rotor and lead to fatigue issues over time. However, since the blades are designed to withstand substantially greater centrifugal loads, these fluctuating aerodynamic loads become a minor concern.

Based on these findings, an overall conlusion could be extracted. Regarding BL generation, it was proven that by following the design implications stated previously, it is physically possible to induce a boundary layer in a wind tunnel with its common characteristics. In what concerns its effects on fan performance, while the observed variations are minimal and could be related to numerical errors, the tendency of the results aligns with previous BLI research. Therefore, to obtain more precise values that would allow for a definitive conlusion on optimizing BLI, the model should be improved or physically implemented.

5.3 Future Work

The results of this study establish a firm basis for future research. As the current tooth configuration effectively reproduces the characteristics of a real-world boundary layer, there is no need to alter its geometry or position. The next logical step would be to build the physical tooth configuration and implement it in a real wind tunnel. This would allow to measure the data and analyze more accurately the effects of BLI on fan perforance, comparing it with the simulation results. Additionally, this would also enable the measurement of acoustic emissions from this fan under BLI conditions and the investigation of noise reduction methods.

On the other hand, future simulations could alter additional parameters in an attempt to improve numerical results. For example, although the current height was established based on typical values for this type of experiments, the impact on fan performance of ingesting a thicker boundary layer could be analyzed. Another possibility could be to increase the tooth's width in order to produce a higher level of turbulence within the boundary layer.

However, it is important to acknowledge that the low operational speeds of the wind tunnel (Júnior *et al.*, 2017) may also be a limiting factor, as the effects of BLI may not be fully reflected as in reality, regardless of the BL's quality. This suggest that future experiments may also obtain better results if conducted in a facility capable of higher speed.

REFERENCES

BHATTACHARYYA JOHN P. ABRAHAM, L. C. J. G. S. Introductory chapter: A brief of an introduction to computational fluid dynamics. *In*: **Applications of Computational Fluid Dynamics Simulation and Modeling**. [*S.l.: s.n.*]: Intech Open, 2022.

COUNIHAN, J. An improved method of simulating an atmospheric boundary layer in a wind tunnel. **Atmospheric Environment**, 1968.

DENG, H. *et al.* Investigation on the inflow distortion of a propulsive fuselage aircraft and its impact on the propulsion fan performance. **Physics of Fluids 1**, 2023.

DIAMANTIDOU D.E.; HOSAIN, M. K. K. R. Advances in boundary layer ingestion technology of evolving powertrain systems. **Sustainability**, v. 14, n. 3, p. 1–55, feb 2022.

DRELA, M. Power balance in aerodynamic flows. **AIAA journal**, 2009.

GUO, R. W.; SEDDON, J. An investigation of the swirl in an s-duct. **Aeronautical Quarterly**, 1982.

H., M.; F., R. Effects of distortion on a bli fan. **The Aeronautical Journal**, 2024.

HALL, D. *et al.* Inlet flow distortion in an advanced civil transport boundary layer ingesting engine installation. **Turbomach**, 2022.

HALL, D. *et al.* Boundary layer ingestion propulsion benefit for transport aircraft. **Journal of Propulsion and Power**, v. 33, p. 1–12, 03 2017.

HARDIN, L. *et al.* Aircraft system study of boundary layer ingesting propulsion. *In*: **48th AIAA/ASME/SAE/ASEE Joint Propulsion Conference & Exhibit**. Atlanta, GA, USA: American Institute of Aeronautics and Astronautics, 2012. p. 3993.

JúNIOR, B. M. *et al.* Baseline acoustic levels of the eesc-usp fan rig. *In*: AMERICAN INSTITUTE OF AERONAUTICS AND ASTRONAUTICS. **2017 AIAA/AAS Guidance, Navigation, and Control Conference**. [*S.l.: s.n.*], 2017.

KAWAI, R. T.; FRIEDMAN, D. M.; SERRANO, L. **Blended wing body (BWB) boundary layer ingestion (BLI) inlet configuration and system studies**. [*S.l.*], 2006.

LEIFSSON, L. **Multidisciplinary Design Optimization of low-noise transport aircraft**. 2006. Tese (Doutorado) — Virginia Polytechnic Institute and State University, 2006.

LIU, X. *et al.* Development and progress in aeroacoustic noise reduction on turbofan aeroengines. **Progress in Aerospace Sciences**, v. 130, 04 2022.

LORD, W. K. *et al.* A performance methodology for ducted boundary layer ingesting propulsion. **AIAA Scitech 2019 Forum**, 2019.

LV, P. *et al.* Performance analysis of wake and boundary-layer ingestion for aircraft design. **Journal of Aircraft**, v. 53, n. 5, p. 1517 – 1526, 2016.

LV, P. *et al.* Performance analysis of wake and boundary-layer ingestion for aircraft design. **Journal of Aircraft**, 2016.

MA, T.; LU, H.; LI, Q. A systematic review of boundary layer ingestion (bli) fan: Current status and future perspectives. **Progress in Aerospace Sciences**, 2025.

MENTER, F. R.; LECHNER, R.; MATYUSHENKO, A. **Best Practice: RANS Turbulence Modeling in Ansys CFD**. [*S.l.*], 2021.

PAN, T. *et al.* A region-segmentation combinational loss model based on data-driven machine learning for a boundary layer ingestion fan. **Aerospace Science and Technology**, 2024.

PARDO, A. C.; HALL, C. A. Aerodynamics of boundary layer ingesting fuselage fans. **Journal of Turbomachinery**, v. 143, n. 4, abr. 2021.

PARDO, A. C.; HALL, C. A. Aerodynamics of boundary layer ingesting fuselage fans. **Turbomach**, 2021.

PLAS, A. *et al.* Performance of a boundary layer ingesting (bli) propulsion system. **45th AIAA Aerospace Sciences Meeting and Exhibit**, 2007.

SANDERS, D. **Boundary Layer Ingestion Performance Assesmentss with Application to Business Jets**. 2018. Tese (Doutorado) — Cranfield University, 2018.

SARKAR, S. **TurboFan engine analysis - design & innovation**. mar. 2006. Tese (Doutorado) — National University Bangladesh, mar. 2006.

SATO, S. **The power balance method for aerodynamic performance assessment**. 2012. Tese (Doutorado) — Massachusetts Institute of Technology, 2012.

SEITZ A., G. C. Parametric design studies for propulsive fuselage aircraft concepts. **CEAS Aeronaut J**, 2015.

SMITH, A. M. O.; ROBERTS, H. E. The jet airplane utilizing boundary layer air for propulsion. **Journal of the Aeronautical Sciences**, 1947.

SMITH, J. W. L. Wake ingestion propulsion benefit. **Journal of Propulsion and Power**, v. 9, p. 74–82, 1991. Disponível em: https://api.semanticscholar.org/CorpusID:123058739.

TANNEHILL, J. C.; ANDERSON, D. A.; PLETCHER, R. H. **Computational Fluid Mechanics and Heat Transfer**. [*S.l.: s.n.*]: Taylor Francis, 1997.

URANGA, A. *et al.* Boundary layer ingestion benefit of the d8 transport aircraft. **AIAA Journal**, 2017.

URANGA, A. *et al.* Analysis of the aerodynamic benefit from boundary layer ingestion for transport aircraft. **AIAA journal**, 2018.

VOIGT, J.; FRIEDRICHS, J. Development of a multi-segment parallel compressor model for a boundary layer ingesting fuselage fan stage. **Energies**, 2021.

WANG, K. *et al.* Behavior of flow distortion within a boundary layer ingestion inlet. **Aerospace Science and Technology**, 2024.

WEI, K. Turbofan and turbojet engines: Working process and future development. **Theoretical and Natural Science**, nov 2023.